Review Article

Syed Muhammad Zain Mehdi[#], Muhammad Faheem Maqsood[#], Alaa Dahshan, Shahbaz Ahmad, Muneeb Ur Rehman, Naesung Lee, Malik Abdul Rehman*, and Muhammad Faroog Khan*

Emerging boron nitride nanosheets: A review on synthesis, corrosion resistance coatings, and their impacts on the environment and health

https://doi.org/10.1515/rams-2024-0075 received June 20, 2024; accepted November 25, 2024

Abstract: The aim of this study is to assess the effectiveness of hexagonal boron nitride (hBN) coatings to enhance the corrosion resistance of metals as well as evaluate their crucial toxicological impacts on both the environment and human health. Organic coatings are extensively applied in the field of protecting metals against corrosion. They are preferred as corrosion inhibitors due to their carbonyl and hydroxyl group content, but they have drawbacks regarding brittleness, porosity, and oxidation susceptibility. In this review, we mainly focused on the synthesis, properties, and applications of hBN coatings and emphasized the

way to improve corrosion resistance in metals and alloys. Furthermore, our discussion demonstrated that the boron nitride nanosheet (BNNS) coatings significantly improve corrosion resistance, hydrophobicity, and crack mitigation properties. The researchers achieved reduced coating porosity and enhanced protection against corrosive media by effectively dispersing BNNS in organic resin. This study also determines the protective mechanism of BNNS composite coatings against corrosion. Moreover, we addressed the impact of BBNS synthesis and its physicochemical properties on the environment and organisms. Finally, suggestions are made for future research and the sustainability of industrial use to broaden the scope of applications for BNNS composite coating.

Keywords: corrosion resistance, barrier coatings, boron nitride nanosheets, environmental and health issues

Syed Muhammad Zain Mehdi, Naesung Lee: Hybrid Materials Centre, Department of Nanotechnology & Advanced Materials Engineering, Sejong University, 05006, Seoul, Republic of Korea

Muhammad Faheem Maqsood: Hybrid Materials Centre, Department of Nanotechnology & Advanced Materials Engineering, Sejong University, 05006, Seoul, Republic of Korea; Materials Science and Engineering Program, College of Arts and Sciences, American University of Sharjah, Sharjah, 26666, United Arab Emirates; Department of Electrical Engineering, Sejong University, 05006, Seoul, Republic of Korea Alaa Dahshan: Department of Physics, College of Science, King Khalid University, Abha, 61413, Saudi Arabia

Shahbaz Ahmad: Materials Science and Engineering Program, College of Arts and Sciences, American University of Sharjah, Sharjah, 26666, United Arah Emirates

Muneeb Ur Rehman: Institute of Metallurgy & Materials Engineering, Faculty of Chemical & Materials Engineering, University of Punjab, Lahore, 54590, Pakistan

1 Introduction

An hBN is a layered structural material that has been investigated for the corrosion resistance coatings due to its high thermal, flame retardancy, and chemical stability [1,2]. Several techniques are reported in the literature, such as galvanization and metallic, which include chromium and nickel coatings in protecting the alloy against corrosion for industrial applications [3-5]. Hot-dip galvanizing is a technique that is mostly used for steel protection that is implanted in soil or concrete [6]. Nonetheless, the problem of white rust, which accumulates on the galvanized layer's steel surface in the atmosphere, adversely affects both the appearance and the properties of galvanized products [7–9]. Anticorrosion coatings, which include chromium coatings, are well-known for their exceptional corrosion resistance properties [10-13], but these coatings are toxic to the environment. Nickel- and copper-based metallic/composite coatings have also been used, but they possess weak durability and wear resistance [14,15]. Furthermore, various corrosion protection coatings have been developed using different

[#] These authors contributed equally to this work and should be considered first co-authors.

^{*} Corresponding author: Malik Abdul Rehman, Department of Chemical Engineering, New Uzbekistan University, Tashkent, Uzbekistan, e-mail: m.abdul@newuzbekistanuniversity.uz

^{*} Corresponding author: Muhammad Farooq Khan, Department of Electrical Engineering, Sejong University, 05006, Seoul, Republic of Korea, e-mail: mfk@sejong.ac.kr

elements, such as cadmium [16], copper [17], and cobalt [18] for marine applications [19] and oceanic transports, but they also result in toxic coatings for the marine ecosystem, which are carcinogenic to humans [20–22].

However, organic coatings are preferred due to a large number of carbonyl and hydroxyl groups, such as phytic acid and tannic acid [23-25]. The carbonyl group presents the carbon double-bonded to oxygen (O=H), whereas the hydroxyl group contains oxygen and hydrogen that are bonded together (OH). Organic coatings contain a relatively thin barrier between the substrate and the environment. There are several organic coatings, such as epoxy, polypyrrole, and acrylic resins that are mostly used for corrosion protection [26-29]. The epoxy resins are diglycidyl ethers of bisphenol A, whereas polypyrrole is the most widely studied among the various types of conducting polymers due to its facile synthesis and promising redox properties. Furthermore, acrylic resin is a type of thermoplastic, which is heated and repeatedly molded to any shape. It is different from epoxy resin due to the re-shaping and manipulation by heat. In addition, organic coatings are brittle, porous, and prone to oxidation. The low evaporation rate, small solid content, and agglomeration are a few of the disadvantages of these types of coatings [30-33]. Adding nanoparticles, such as tantalum carbide, hafnium carbide, cerium oxide, and other metal oxides, can provide favorable effects on the anticorrosive properties. Better mechanical properties of organic coatings can be achieved even at low loads depending on the particle morphologies, surface energies, and the inherent small sizes of the particles [34-37]. However, these types of nanoparticles lack non-toxicity, high thermal stability, and lubricity. hBN provides better chemical inertness, thermal stability, and lubricity, which contrasts with the previously mentioned nanoparticles. This makes it a more effective anticorrosion coating material. Moreover, the non-toxicity and low density of hBN offer advantages for anti-corrosion applications. The hBN has recently been studied, improving the corrosion resistance of metals and alloys for these reasons [38-40].

An extensive amount of research has been conducted on graphene, and hBN is relatively new in regard to corrosion protection [1,41,42]. The hBN is gaining a lot of attention due to corrosion protection due to its outstanding chemical and physical properties, which include high hardness, oxidation resistance, insulating properties, corrosion resistance, low density, and barrier protection [43–47]. Nadeem *et al.* [48] found that the corrosion resistance of mild steel increases six times by BNNS coating, which improves its hydrophobicity, inertness, an increased polarization of charge distribution, and dielectric nature [49]. Cui *et al.* [20] added hBN into epoxy resin to enhance

corrosion protection and crack mitigation properties. This improvement was achieved due to the effective dispersion of the hBN that interrupts the crack propagation as well as also causes a reduction in the coating porosity, which inhibits the penetration of the corrosive medium in epoxy resin.

This review investigates the effectiveness of BNNS coatings, cultivating the corrosion resistance of metals and alloys by comparing the surface morphology of BNNSs that are synthesized by various methods using scanning electron microscopy (SEM), and the corrosion inhabitation mechanism of BNNS coatings. In addition, we highlighted the ecological and human health risk assessments of the possible hazards and risks of BNNS materials.

2 Literature review

2.1 hBN

hBN is a crystalline compound of boron (B) and nitrogen (N) that has the chemical formula arranged hexagonally like a honeycomb structure analogous to graphene. It is a colorless crystalline material that has covalent bonds between B and N. There is a more energetically stable and favorable B–N bond than B–B and N–N bonds. hBN is mostly compared with carbon allotropes [50]. It is a chemically and thermally resistive refractory compound. It is a synthetic compound that can be produced using multiple methods [51]. Figure 1 illustrates the chemical structure of hBN.

2.1.1 Properties of hBN

hBN is a two-dimensional material, which has garnered a considerable amount of consideration in recent years due to its rare properties and potential applications in various materials science fields. The band structure of hBN is analogous to graphite, which is described by its layered hexagonal lattice arrangement of boron and nitrogen atoms. This structure reveals several outstanding properties, which maintain its structural integrity at high temperatures as a result. This further enhances its usage in high-performance applications. The following are a few more properties of hBN and BNNS.

- The band gap is 6.8 eV, and hBN acts as a thermal conductor and electrical insulator as a result [52].
- The low density is theoretically about 2.27 g·cm⁻³.
- They are against thermal shocks.
- The multi-layers act as a lubricant [53].

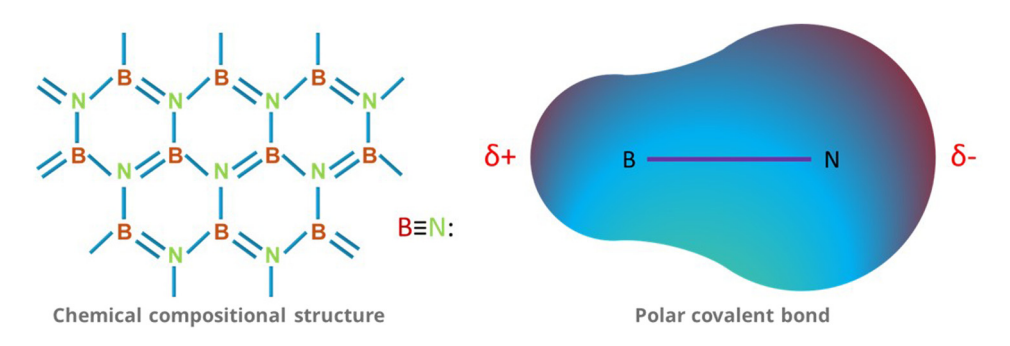


Figure 1: Chemical compositional structure and polar covalent bond of hBN.

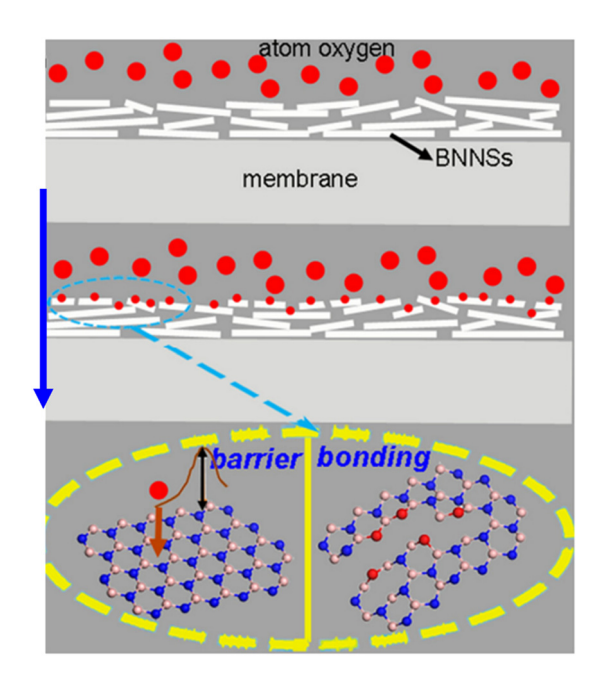


Figure 2: Illustration of the mechanism where BNNS coating can shield the polymer from oxygen-atom corrosion [59].

- They have mechanical properties and high thermal conductivity [54].
- · The high thermal stability and bending modulus are 18-32 GPa [55,56].
- The thermal conductivity is about 1,700–2,000 W⋅mK⁻¹ [57].
- · They have good oxidation and corrosion resistance.
- They have stability at high temperatures near 2,600°C.

- They are chemically inert due to sp² covalent bonds and corrosion resistive.
- The in-air stability is up to 1,000°C.
- They have better dielectric properties than graphene, so they are useable in places where graphene cannot be used [58].
- The act as a barrier between the environment and the substrate's surface, which is illustrated in Figure 2.

Furthermore, the optical properties of hBN also get attention due to a wide energy bandgap that allows for its potential use in the optoelectronic devices of solar cells and photodetectors. The unique combination of mechanical strength, chemical stability, and optical properties largely enables the hBN to be a versatile material for diverse next-generation technology.

We essentially include a relative analysis, which is displayed in Table 1, and it highlights the properties of hBN compared with other metal nitrides to illustrate the superior properties of hBN and its potential applications. This comparison will be constructive to understand the advantages of hBN in regard to various perspectives of anti-corrosion.

2.1.2 Applications of hBN

hBN is an outstanding material with a variety of applications in several industries due to its exceptional properties. It possesses excellent thermal conductivity, and it is

Table 1: Comparison study of hBN with other metallic nitrides [60-62]

Properties	Materials			
	hBN	TiN	AIN	VN
Thermal conductivity Electrical conductivity Chemical inertness Lubricating properties	High Insulating Highly inert, resistant to acids and bases Excellent, low friction	Low Conductive Moderately resistant Poor	Low Conductive Moderately resistant Poor	Low Conductive Highly resistant Poor

important to note that boron nitride (BN) has a wide energy bandgap that acts as an electrical insulator and not a conductor. This type of combination of high thermal conductivity and high resistivity makes it a fascinating candidate in the field of electronic applications. hBN is generally used as a heat sink in computer chips and light emitting diodes, which efficiently prevents overheating and thereby improves the performance to ensure the durability of electronic devices, in electronic devices. hBN also has an application beyond electronics, such as being used as a lubricant specifically in harsh environments where high temperatures are implicated. The high thermal stability also ensures its crucial role as a solid lubricant in the aerospace and automotive manufacturing industries. hBN is in the realm of anti-corrosion coatings as applications due to its resistance to heat and chemicals, which makes it suitable for protecting instruments and equipment in critical environments, such as those that are encountered in metalworking. A few more promising applications are highlighted below.

- hBN is used in electronic components, such as coil forms, substrates, and prototypes.
- hBN is used in semiconductor processing as boron wafers in silicon.
- hBN is used in vacuum-melting crucibles and highly precise sealing and brazing.
- hBN is used in high-temperature furnace supports and fixtures [63].

2.1.3 Synthesis of hBN

The synthesis of hBN earned a significant amount of attention in materials chemistry due to its special properties, such as high thermal conductivity and mechanical strength. BN has an analogous structure to carbon, which is due to the arrangement of boron and nitrogen atoms in a hexagonal lattice. hBN was first synthesized by *Balmain* in 1842 as a product of potassium cyanide and boric acid, but the composition was not stable. *Ventorf* succeeded in 1957 in regard to producing cubic hBN at a high temperature and pressure and named the product *Borazon* [53,64].

There are numerous synthesis methods for BN, and each of them has distinct advantages and limitations. The most common method is the reaction of boron oxide (B_2O_3) or boric acid (H_3BO_3) with ammonia (NH_3) at high temperatures in a furnace tube under an inert atmosphere, such as nitrogen gas to avoid the oxidation of hBN. Another method is the reaction of boron halides, such as boron trichloride (BCl_3) , which includes ammonia or hydrazine (N_2H_4) at high temperatures. These reactions typically

result in the formation of hBN, which has a layered structure like graphite.

In addition, another technique in regard to synthesizing cubic BN (c-BN) has a diamond-like structure. This technique of synthesizing c-BN requires high-pressure high-temperature processes, which imply boron and nitrogen precursors to extremely high pressures and temperatures in a diamond anvil cell or cubic press. Finally, the chemical vapor deposition (CVD) method, where boron and nitrogen precursors are thermally decomposed onto the substrate at high temperatures, deposits a thin c-BN film.

The synthesis of hBN is generally an intricated and multi-step process that involves careful control of reaction conditions and precursor materials. The research community continues to explore the prospective applications of hBN by establishing novel synthesis methods and techniques, which could be more advanced in the field of hBN materials science.

2.1.4 Types of hBN

BN is a polymorphic compound that exists in different forms, such as hBN, a-BN, t-BN, m-BN, r-BN, w-BN, o-BN, and c-BN, which are displayed in Figure 3 [66]. BN has three allotropes in translucent form that include sphalerite BN (β -BN), which is like a cubic diamond, hBN, which is similar to graphite, and wurtzite BN (γ -BN), which is similar to a hexagonal diamond. According to dimensions, fullerene-like (single-layered octahedral) forms are 0D in structure, nanotubes and NTs are 1D in structure, hBN is 2D in structure, and cubic BN is 3D in structure [67]. c-BN and hBN are the most common types of hBN among all these forms. hBN is the most stable form, which is known as white graphene.

2.2 BNNSs

hBN is the most stable form of hBN, which is also known as *graphitic boron nitride* or *white graphite*, due to its resemblance with graphite. It has a similar layered structure to graphene. Boron and nitrogen atoms are bonded together through a covalent bond, and interplanar layers of BNNS are held together through the weak Van der Wall forces, which are shown in Figure 4. Nitrogen and boron atoms attract each other due to electronegativity differences between them and form ionic characters [69]. The angle is 120° between N–B–N or B–N–B. A single layer of hBN is known as a *BNNS* [70]. hBN can be produced by reacting with urea–boric acid, melamine–boric acid, and

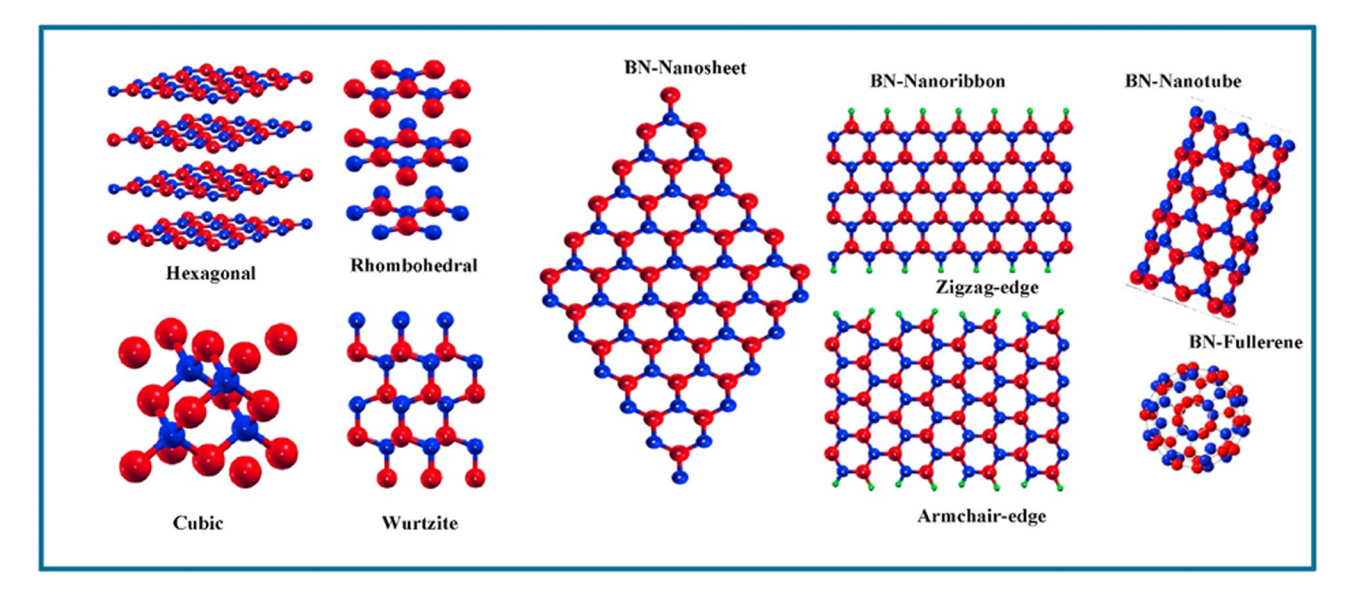


Figure 3: hBN structures of different types and dimensions [65].

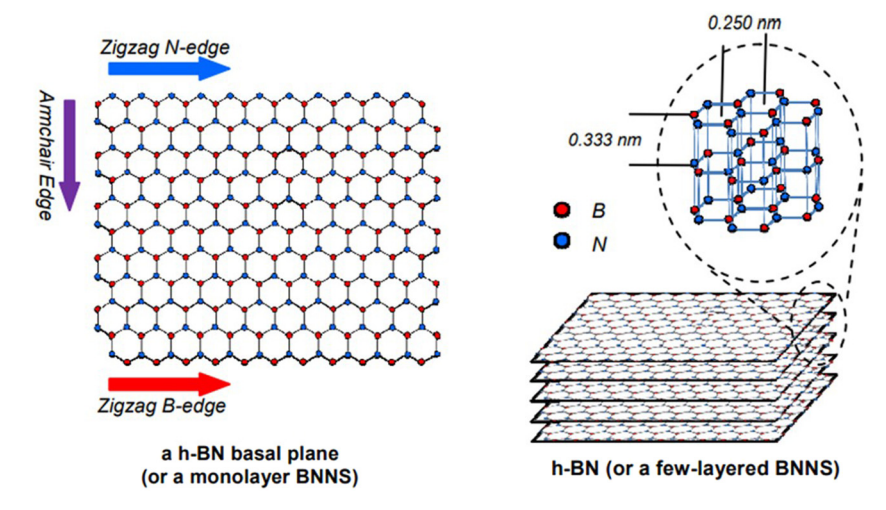


Figure 4: Schematic illustration of BNNS structure [68].

melamine-urea and boric acid precursors, which is followed by the pyrolysis and heat treatment in a nitrogen atmosphere at 1,050°C [71].

2.2.1 Synthesis of BNNS

Since BNNS consists of a monolayer of hBN, so several exfoliation methods are used for the production of BNNS. There are several methods for the synthesis of BNNS, and a few of them are mentioned in Figure 5. Moreover, we established a comparison study, which is provided in Table 2, to enhance the comprehension of the advantages and disadvantages of the BNNS synthesis routes.

- The exfoliation method (liquid/chemical) [74].
- The CVD method [10].
- The directional etching method [75].
- The mechanical cleavage method [76].
- The electron beam (high energy) method [77].
- The wet chemical synthesis method [78].
- The microwave-assisted synthesis [79].

We only discuss the first two methods, which are related to the top-down and bottom-up approaches, after this point.

2.2.1.1 Liquid exfoliation method

It is a simple method that is based on the top-down approach, in which the inter-layers of cohesion of a bulk

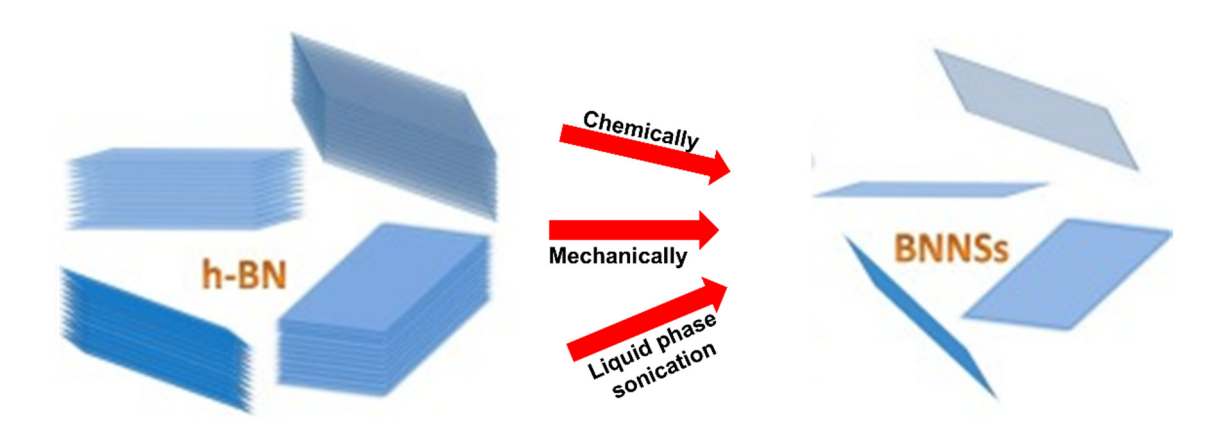


Figure 5: Schematic representation of the various synthesis methods of BNNS from bulk hBN.

Table 2: Comparative analysis of various synthesis methods for BNNSs [72,73]

Synthesis methods	Advantages	Disadvantages
Mechanical exfoliation	Simple, low-cost, highly crystalline	Low production yield
Chemical weathering	Low cost, tunable number of layers and morphology	High defect concentration
CVD	High-quality, large-area BNNSs	High cost, special catalyst, and substrates required
Physical vapor deposition	High quality, tunable morphology, and thickness	High vacuum, high cost
Liquid exfoliation	Precise control dimension of the nanosheets	Utilizes toxic chemicals and surfactants

hBN precursor are broken down to produce BNNS by using different solvents.

- Zhi et al. [80] produced BNNS by sonicating micron-sized hBN particles in N-dimethyl formamide solvent for 10 h by using a probe-type sonicator. As a result, 1–5 nm thick BNNSs are produced.
- Wang *et al.* [81] produced 2 nm thick BNNS through the exfoliation of micron-sized hBN in methane sulfonic acid and 8 h of ultra-sonication.
- Marsh et al. [82] produced 7–9 nm thick BNNS by the sonication of bulk hBN in a solvent containing 60 wt% tert-butanol in water.
- Thangasamy and Sathish [83] produce BNNS by sonicating in a mixture of isopropanol-water for 5 min.

2.2.1.2 CVD method

It is a bottom-up approach method that proceeds at high temperatures in the presence of precursors that are boron rich such as borazine, ammonia borane, or boron oxide, which can decompose in a nitrogen environment.

• Gao *et al.* [84] produced 25–50 nm-thick BNNS using melamine (powder) and B_2O_3 as precursors by mechanically mixing them. This was followed by placing them in a CVD furnace for 1 h at a temperature that ranged from 1,100 to

- 1,350°C in an Ar and nitrogen environment, which is shown in Figure 6.
- Nadeem et al. [85] produced 5–11 nm-thick BNNS in a CVD at a temperature that ranged 900–1,400°C at a heating rate of 50°C·min⁻¹ for 1–9 h. About 1–2 μm pure boron powder was used as a precursor in a nitrogen environment.

2.2.1.3 SEM analysis of the produced BNNS

The SEM analysis of hBN synthesized *via* various routes is given in Figure 7. Figure 7a and b shows SEM images of hydrothermally exfoliated BNNS with rough and irregular morphology forming agglomerates. Figure 7c and d shows SEM images of CVD-grown hBN that represent a dense and uniform array of hBN nanoparticles. The SEM images of hBN grown *via* the wet chemical route are provided in Figure 7e and f, which represent rod-like morphology with clear and elongated hBN tubes, whereas hBN that is grown using the freeze casting method shows fibrous and layered texture. This indicates a network or interconnected structure, which is shown in Figure 7g and h. It is essential to understand the morphological variety of materials at various sizes and processing circumstances to customize

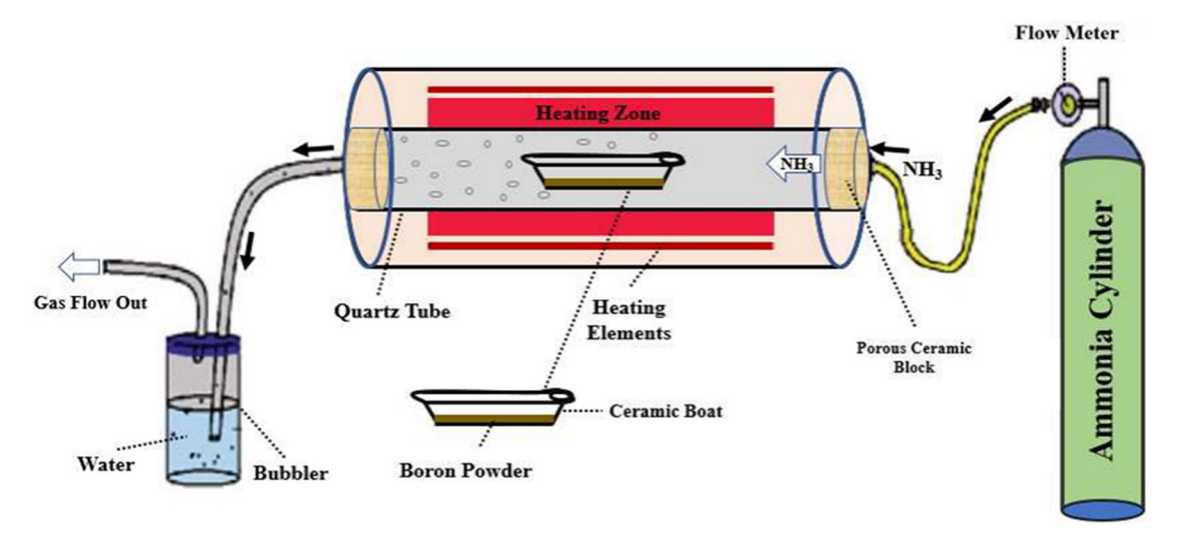


Figure 6: Schematic CVD apparatus drawing for BNNS production [85].

the hBN characteristics for applications, which is demonstrated by the SEM images [74,86–88].

2.2.2 Applications of BNNS

Some of the common applications of BNNS are stated as follows.

- BNNS can be used in dielectric applications due to its insulating nature [89].
- BNNS can be used as a photoluminescent material [90].
- BNNS can be used in thermal interface applications [91].
- BNNS can be used as a nanofiller in composites due to its mechanical properties [92].
- BNNS can be used as a water repellant [46].
- BNNS can be used for anti-fouling [93,94].
- BNNS can be used as an anti-corrosion system [47].
- BNNS can be used as a solid-state lubricant [95,96].
- BNNS can be used for water cleaning [97].

We discuss some of the previous studies where BNNS is used as the main component in anti-corrosion coatings in the following sections.

2.3 hBN in anti-corrosion coatings

Ysiwata-Rivera *et al.* [98] prepared functionalized hBN with polyacrylic acid plasma polymerization. Rheometric testing and zeta potential were conducted to check the stability and viscosity of the nanocoating. The 1 wt% coating showed a twofold increase in magnitude corrosion resistance compared to pure acrylic paint. The Nyquist diagram

for the 304-SS and the coating made of acrylic resin is shown in Figure 8a. A typical steel curve line for 304-SS is shown in this graph, and two semicircles of varying sizes are shown in the acrylic resin. The Bode-impedance data are displayed in Figure 8b, which is where it is shown that 304-SS has the lowest impedance value over the complete frequency range. It was found that coatings that contain untreated BNNS have a somewhat greater low-frequency impedance than coatings that contain modified nanoparticles. The EIS bode plot in Figure 8b shows low-frequency unmodified hBN $|Z| = 1.52 \times$ $10^9 \,\Omega \cdot \text{cm}^2$, modified hBN $|Z| = 5.75 \times 10^8$, and acrylic resin | $|Z| = 8.40 \times 10^6$. The impedance value increases with an increase in the hBN concentration without plasma modification. The Warburg impedance value at 1 wt% for unmodified hBN was 9.30×10^7 , and it was 5.32×10^8 for modified hBN.

Fan et al. [45] prepared a corrosion-resistant coating of acrylic resin with modified BNNS on a hot dip galvanized steel substrate. The BNNSs were prepared by adding 1 g of hBN powder and 0.5 g of potassium permanganate in 200 mL of deionized water with a small amount (30 mL) of sulfuric acid under continuous stirring for 12 h. The suspension was prepared with 20 mL of hydrogen peroxide, and it was centrifuged at 3,000 rpm. The supernatant was then filtered, washed, and dried. About 0.6 g of the BNNSs with 0.16 g of the buffer solution were added into 100 mL of ethanol for the modification, and it was sonicated for 30 min. Dopamine hydrochloride (0.24 g) was added to the mixture, and it was stirred for 6 h. The modified BNNs obtained are PDA/BNNS. One milliliter of KH560 (3-glycidoxypropyltrimthoxysilane) was added to this solution, and it was placed for 5 h at 60°C. The solution was filtered and washed with deionized water and ethanol and

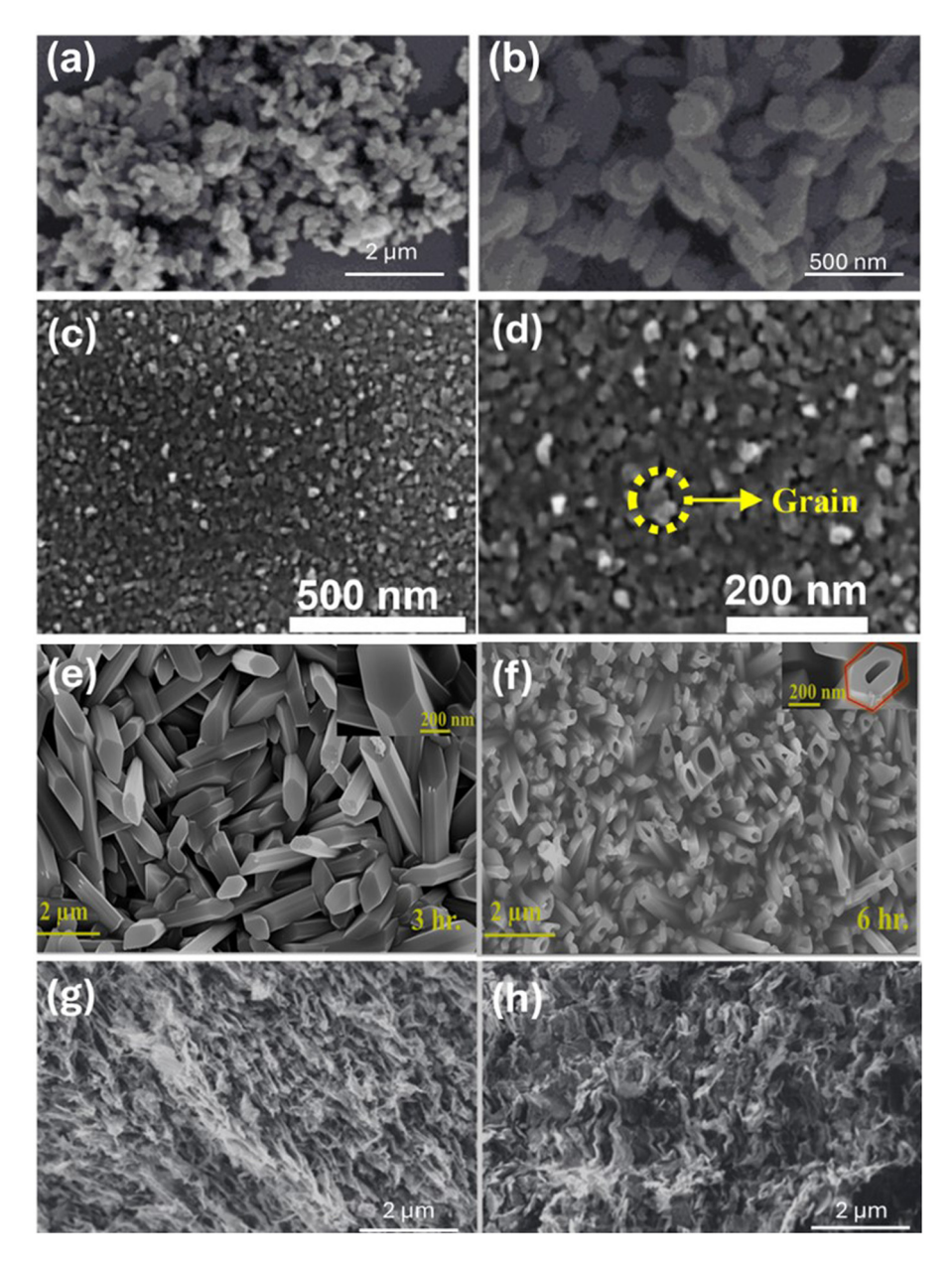


Figure 7: A morphological analysis of the SEM images of hBN synthesized *via* (a and b) hydrothermal exfoliation, (c and d) CVD, (e and f) the wet chemical route, and (g and h) the freeze casting method [74,86–88].

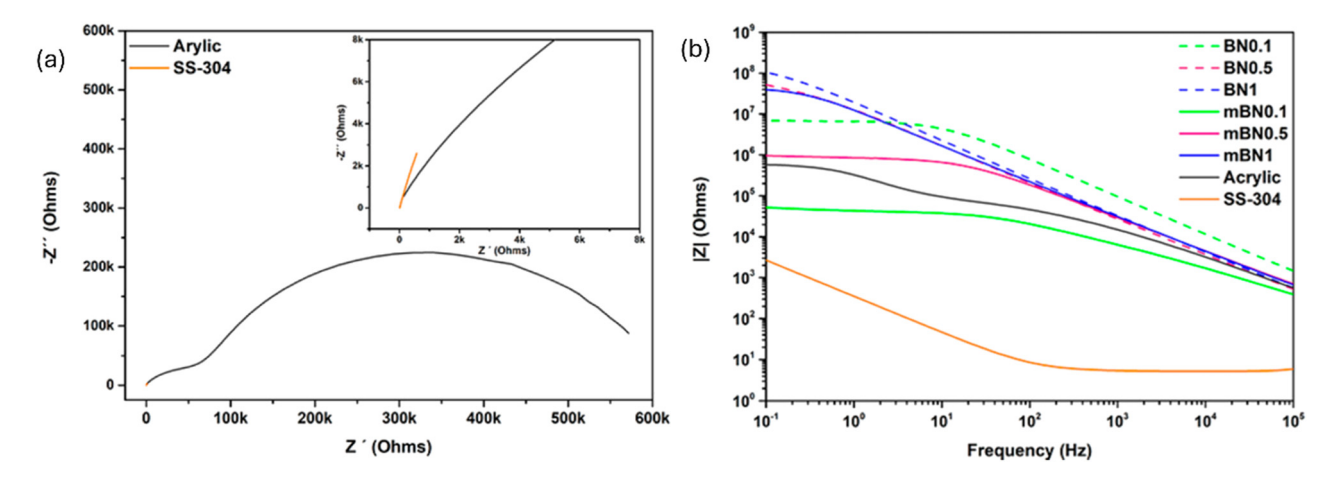


Figure 8: (a) Nyquist plot for different samples and (b) the impedance vs frequency graph [98].

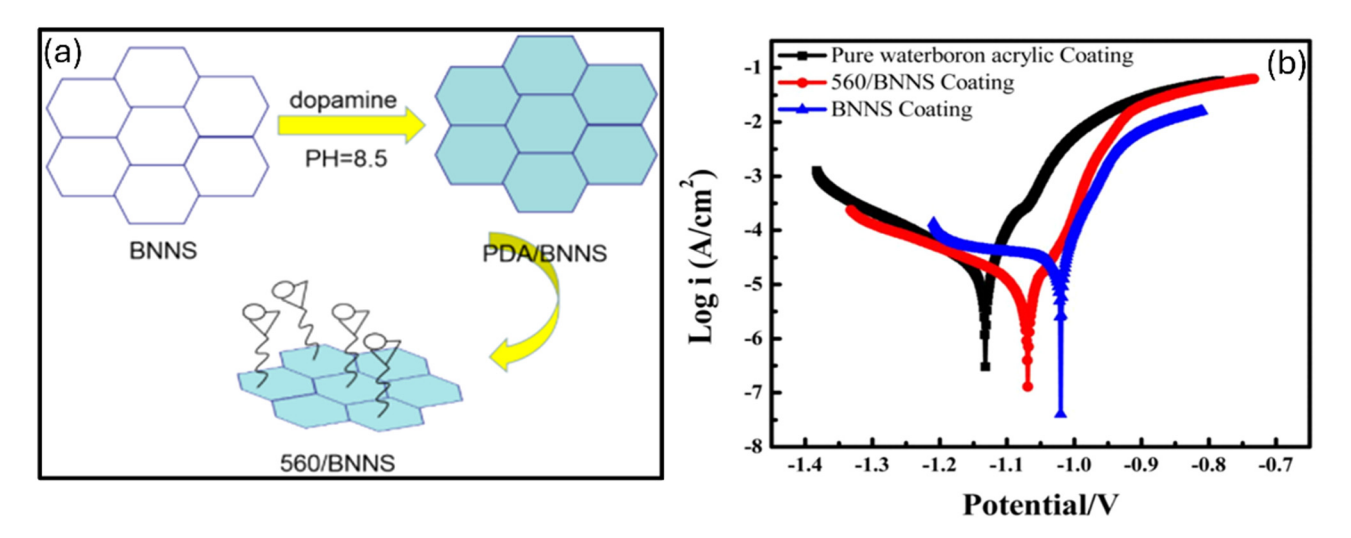


Figure 9: (a) Schematic diagram of modified BNNS (560/BNNS) and (b) potentiodynamic polarization curves of a pure water-borne acrylic coating, BNNS coating, and 560/BNNS coating [45].

vacuum dried. The modified BNNS prepared was 560/BNNS, which is shown in Figure 9a.

The tannic acid (0.3 g) solution was prepared in 200 mL of deionized water for the anti-corrosion coatings. IFC (polyoxymethylene ether) 0.1 g, (1-hydroxyethane-1,1-diphosphonic acid) HEDP (0.1 g), and OP (0.1 g) were added to the prepared solution. Forty grams of the water-borne acrylic solution and 0.02 g of the modified BNNS were added into the above solution, which was stirred continuously. Galvanized steel was dipped into the above solution for 20 s, washed with deionized water, and dried naturally. The Tafel polarization was performed in a 3.5% NaCl environment for corrosion resistance. Figure 9b shows that the current density of the acrylic resin decreased from 2.3×10^{-7} to 2.2×10^{-5} A·cm⁻² after the addition of modified BNNS. The anticorrosion coating with modified BNNS showed an impedance of 4,435 Ω·cm². This impedance is higher than BNNS 2,500 Ω·cm² and acrylic resin $1.500 \,\Omega \cdot \mathrm{cm}^2$.

Huang *et al.* [99] prepared zinc phosphate BNNS coatings for anti-corrosion purposes on mild steel. The mild steel was prepared by removing rust from the surface using SiC paper. The substrate was cleaned by dipping it in a sodium hydroxide (NaOH) solution to remove organic material, and it was then rinsed with deionized water and dried in air. The phosphate bath that contained hBN was prepared by constantly stirring it for good dispersion of hBN. The prepared mild steel samples were then immersed in a bath for 20 min at 40°C, which is revealed in Figure 10a. The sample was cleaned with deionized water to remove acids and salts from the surface after immersion. The samples were then dried and placed in a drying vessel for characterization. There are five different compositions of hBN

coatings that were prepared, which include hBN-0 (0 g·L⁻¹), hBN-0.15 (0.15 g·L⁻¹), hBN-0.30 (0.30 g·L⁻¹), hBN-0.45 (0.45 g·L⁻¹), and hBN-0.60 (0.60 g·L⁻¹). Three characterization techniques were used for the corrosion resistance. The Tafel polarization plots in Figure 10b show that the curve of the hBN containing samples moved toward the right side compared to the simple phosphate coating. The phosphate coatings showed high corrosion rates. The thick and dense hBN coatings showed high corrosion resistivity and the barrier effect. hBN-0.45 showed 5334.44 Ω ·cm² corrosion resistance, and hBN-0 showed 523.30 Ω ·cm², which is 1 order of magnitude less than hBN-0.45. The EIS measurements were taken at room temperature based on the phase angle, Bode, and Nyquist.

According to the Nyquist plot, which is displayed in Figure 10c, the diameter of the semicircular shape that represents phosphate increases with an increase in the amount of hBN, which shows an increase in the charge transfer resistance. Furthermore, the Bode plots in Figure 10d and e show that high phase angle and high frequency were achieved for all hBN that contained phosphate coatings, such as hBN-0.45, which means that the phosphate coating intactness increases after the addition of hBN, and the cathodic delamination of the phosphate crystals decreases. According to the Bode impedance, hBN-0.45 showed the highest impedance $2.01 \times 10^3 \ \Omega \cdot \text{cm}^2$ at a low frequency compared to hBN-0, which was $9.71 \times 10^1 \ \Omega \cdot \text{cm}^2$.

Zhang *et al.* [100] developed a filler hBN@F-SiC for the anticorrosion coatings. This filler was introduced in epoxy to see the effect on corrosion resistance properties. SiC was hydrophobically modified by introducing –OH on the surface using the chemical drafting method for F-SiC. Modified SiC (0.4 g) with 100 mL of ethanol was magnetically stirred

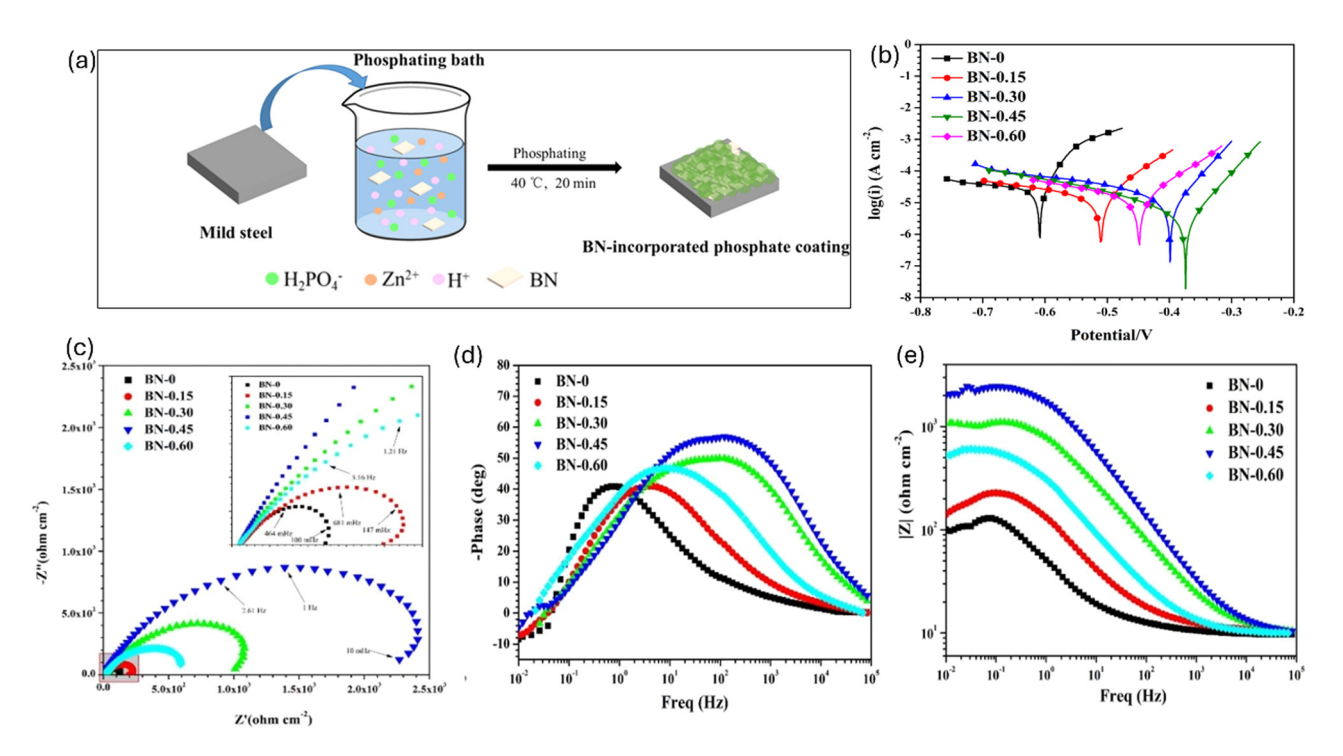


Figure 10: (a) Schematic presentation of introducing BN in phosphate coating and (b) potentiodynamic polarization curve of phosphate coatings, and the EIS measurements, which include (c) the Nyquist plot, (d) the phase angles, and (e) the Bode impedance [99].

that included the dropwise addition of glacial acetic acid until 4-5 pH was reached, which is shown in Figure 11a. Ultrapure water with 0.8 g of 1H,1H,2H,2H-trifluorotrifluoro-n-octyltriethoxysilane was added to the mixture to react for 2 h at 500 rpm and 70°C temperature. The mixture was dried for 12 h at 80°C to produce F-SiC powder. hBN-OH was prepared by adding 0.1 g of hBN in 5 M NaOH and stirring it for 8 h at 125°C for complete dispersion. hBN-OH was obtained after centrifuging and drying the mixture. The final step was the hBN@F-SiC synthesis. Modifier y-amino propyl triethoxy silane (KH550) was added in 0.2 g of F-SiC, sonicated for 30 min, and stirred for 4 h at 70°C to get grafted F-SiC. Grafted hBN-OH is obtained the same as F-SiC by adding (glycidoxy-propyltrimethoxysilane) KH560 in hBN-OH. Three mass ratios of mBN:mF-SiC were made, which included 3:1, 2:1, and 1:1. mBN and mF-SiC were sonicated for 30 min in the presence of anhydrous ethanol for the preparation of hBN@F-SiC. The mixture was dried and hBN@F-SiC was obtained after stirring for 4 h. Q235 steel was stand-blasted to remove the rust. hBN@F-SiC was added and mixed in CYD-014 with epoxy resin in the ratios of 3:1, 2:1, and 1:1. Magnetic and ultrasonic stirrers were used for mixing. The coatings were placed in a vacuum to remove the bubbles. A wire coating machine of 60 µm was used to coat the substrate's surface. Dynamic polarization and salt spray tests showed exceptional corrosion resistance. hBN@F-SiC/ EP (2:1) showed more than $10^{10} \,\Omega \cdot \text{cm}^2$ of impedance, which is 10^3 times higher than pure EP coating, at a low frequency ($10^{-2} \,\text{Hz}$) and 400 h of soaking in 3.5% NaCl, which is revealed in Figure 11b and e.

Zou *et al.* [101] succeeded in regard to developing a plasma-treated hBN nanoflakes coating in an acrylic matrix. Figure 12 shows that a homemade plasma chamber was used to attain low plasma pressure to prepare modified hBN nanoflakes.

A 2.45 GHz microwave was used as the source in the plasma treatment. The processing pressure was 1–100 Pa at 800 W microwave power. About 0.5 g hBN was placed in a chamber within a petri dish for 3 min of the plasma treatment. Three types of gases were used in the plasma chamber, which included (4:1) Ar + NH₃, (4:1) Ar + H₂, and Ar. The plasma-treated 0.3 g hBN nanoflakes were added to acrylic resin (30 mL). The mixture was mixed for 20 min in a high-speed homogenizer for the dispersion. Ten to fifteen drops of deformer, a 0.5–1% leveling agent, and an antiflash rusting agent were added in the last 10 min of the dispersion. A 150 µm-thick coating was applied on a low-carbon steel substrate by using a rod coater. The coating was dried at room temperature before starting the characterization. According to the potentiodynamic polarization results in Figure 12b, the untreated hBN showed the highest current density about 4.990 × 10⁻⁵ μA·cm⁻². hBN treated in

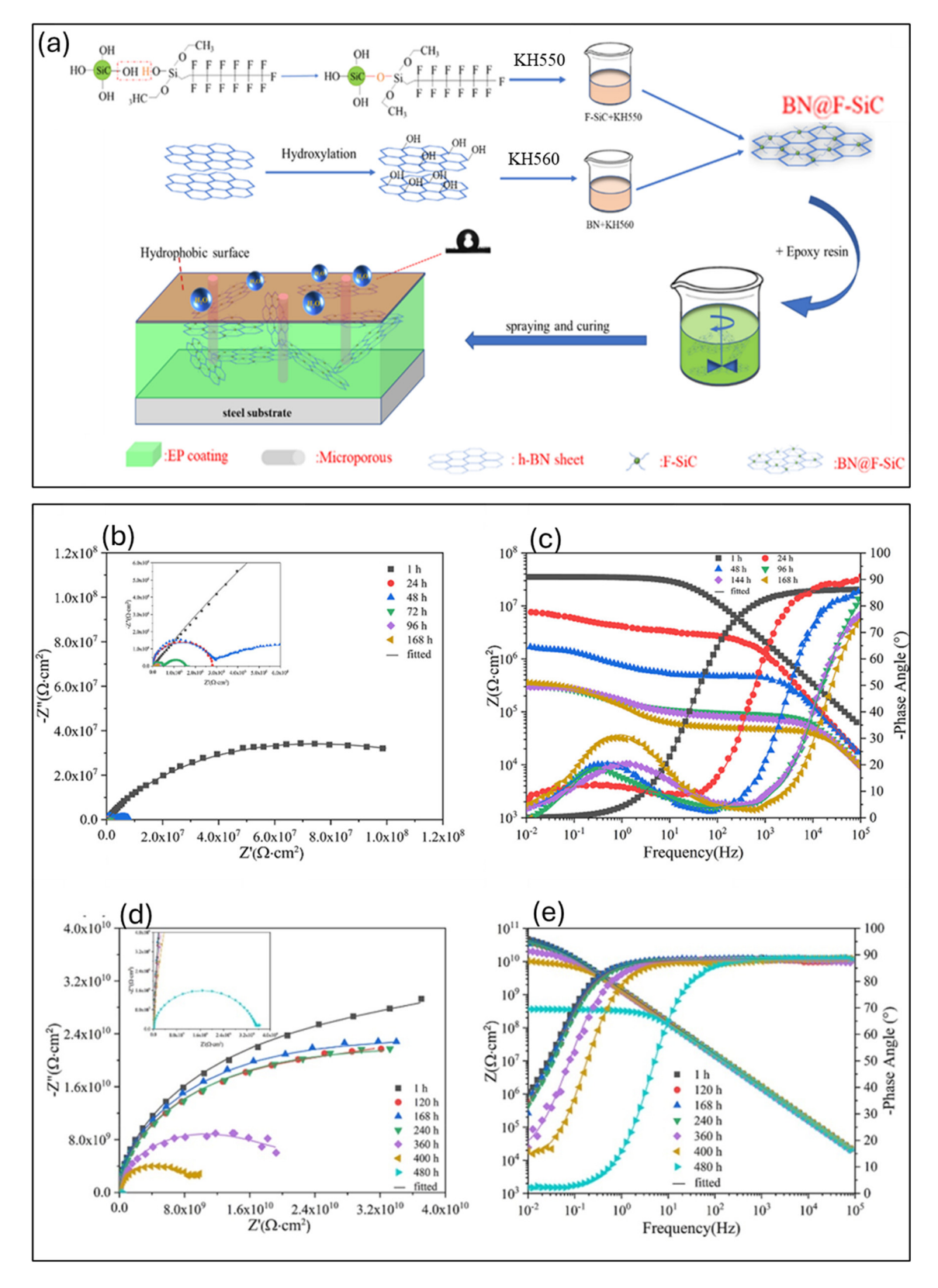


Figure 11: (a) Schematic presentation of preparing a composite coating, the Nyquist and Bode diagrams of (b and c) pure BN and (d and e) BN@F-SiC (2:1)/EP soaked in 3.5% NaCl for different times [100].

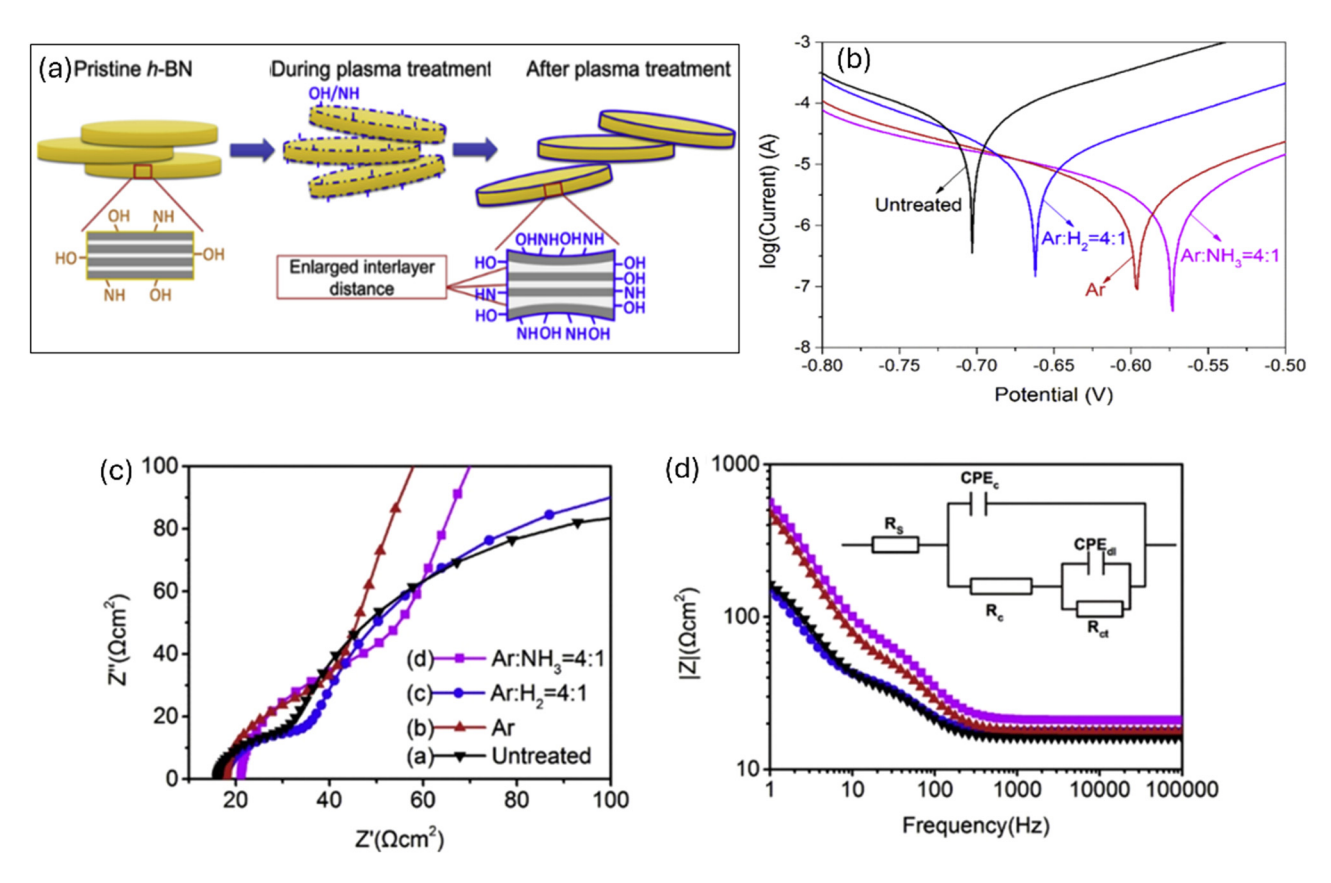


Figure 12: (a) Schematic representation of changes in hBN after the plasma treatment, (b) potentiodynamic polarization curves, (c) EIS measurements and Nyquist plots, and (d) the Bode impedance plots. The inset shows the equivalent circuit. The electrolyte resistance is represented by R_{cs} , the coating resistance by R_{cs} , the charge transfer resistance by R_{cs} the coating capacitance by CPEc, which is the capacitance between the substrate and the electrolyte, and the Warburg impedance by CPEdI [101].

Ar-NH₃ showed a minimum current density of 3.834×10^{-6} μA·cm⁻², which was 13 times less than the untreated hBN coating. The corrosion potential moved toward the positive side after plasma treatment, which is revealed in Figure 12b. The larger semicircle is shown by Ar–NH₃, which is shown in Figure 12c, in EIS Nyquist plots. According to the Bode plots, the Ar-NH₃-treated samples showed the best results in all the coatings at both low and high frequencies, which are illustrated in Figure 12d. The inset of Figure 12d presents the equivalent electrical circuit. However, two things were focused on after setting the Randles-Warburg model's parameters, which included the charge transfer resistance (R_{ct}) and the coating capacitance (CPE $_c$). If the coating R_{ct} value is high and the CPE_C value is low, it means that the coating has good corrosion resistance properties. CPE_C shows water take-up capacity, and R_{ct} shows resistance against aggressive and harmful species [102-104]. All plasma-treated coatings showed high R_{ct} and small CPE_c values. Ar-NH₃ showed the smallest CPE_c value of 6.58×10^{-5} F·cm⁻² and the highest $R_{\rm ct}$ values of 7.37 × 10² Ω ·cm², and these values are 22 times lower (1.53 × 10^{-3} F·cm⁻²) and 3.6 times higher (1.60 × 10^{2} Ω ·cm²) than the untreated hBN, respectively.

A graphic representation, which is illustrated in Figure 13a, shows polypyrrole-functionalized BNNSs. Sodium dodecylbenzene sulfonate was utilized as a dispersion agent in a water–ethanol solvent to reduce the BNNS agglomeration as well as regulate the degree of pyrrole crosslinking during polymerization. Pyrrole was *in situ* polymerized on the BNNS surface with the addition of $(NH_4)_2S_2O_8$ *via* the π - π interactions between the aromatic pyrrole molecules and the hexagonal rings of BNNS. The optical images of the f-BNNS (0.7 mg·mL^{-1}) and the as-exfoliated BNNS (0.7 mg·mL^{-1}) dispersion in ethanol show that the f-BNNS was quite stable after 24 h of standing, which is displayed in Figure 13b. On the other hand, the as-exfoliated BNNS precipitated during the same standing time without polypyrrole functionalization.

The open-circuit potential (OCP) values of the f-BNNS0.5/ EP and f-BNNS_{0.5}-PPyz/EP coatings are shown in Figure 13d, which follows the specific day of immersion in a 3.5% NaCl

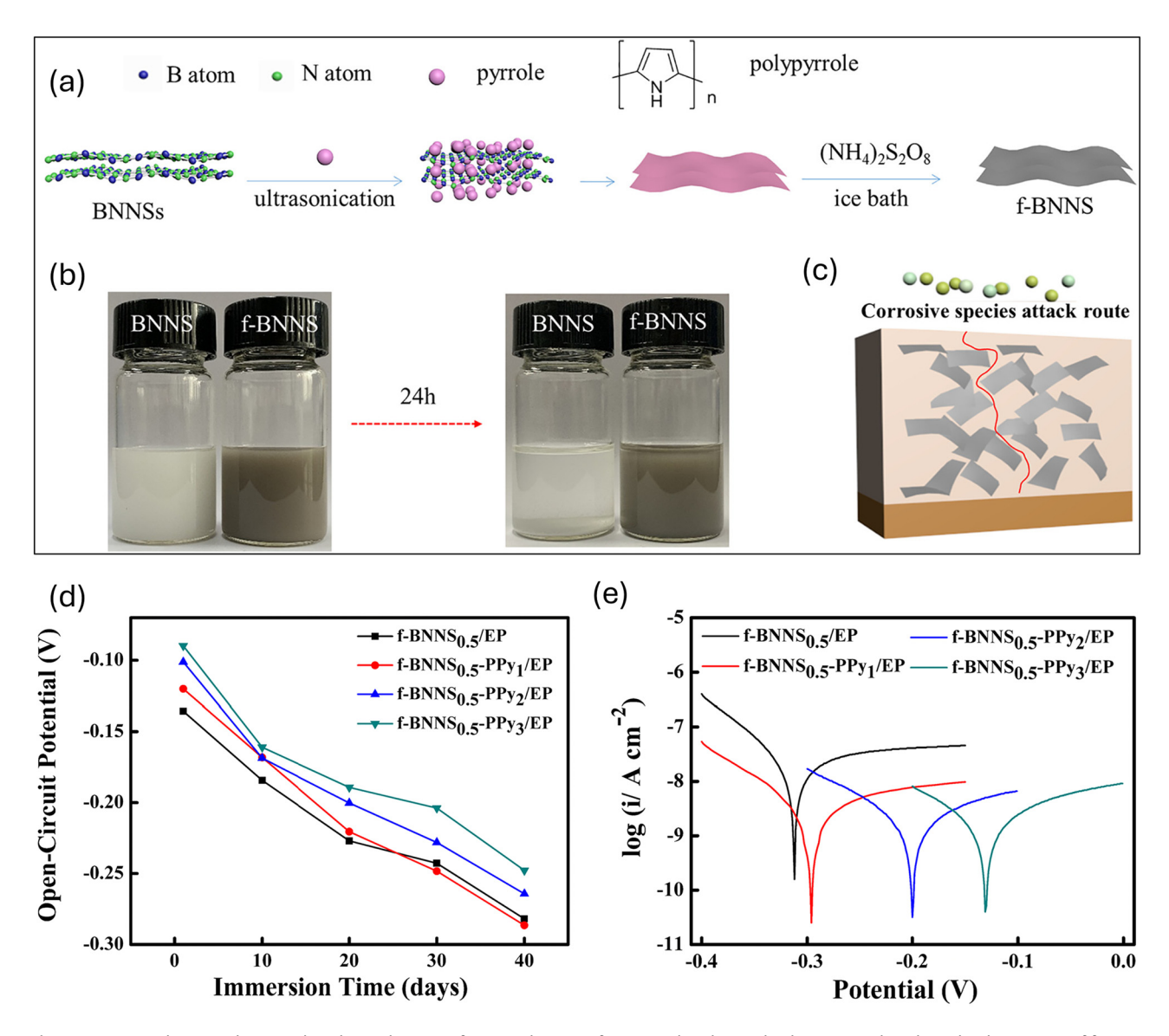


Figure 13: (a) A schematic diagram that shows the *in situ* functionalization of BNNS with polypyrrole, (b) pictures that show the dispersions of f-BNNS and as-exfoliated BNNS in ethanol, (c) an example of composite coatings' ability to resist corrosion, (d) OCP, and (e) potentiodynamic polarization of substrate coated with f-BNNS_{0.5}/EP, f-BNNS_{0.5}-PPy₁/EP, f-BNNS_{0.5}-PPy₂/EP, and f-BNNS_{0.5}-PPy₃/EP coatings [29].

solution. A high OCP value often indicates a low corrosion tendency. The OCP values of the f-BNNS_{0.5}-PPyz/EP coatings (z=1,2, or 3) positively increase as the polypyrrole content increases, which indicates that polypyrrole effectively blocks the infiltration of corrosive species onto the underlying metal. The corrosion potential ($E_{\rm corr}$) is unaffected by the electrical resistance of the coating, so it may be a reliable indicator of the state of corrosion on coated metal. Steel is well protected against corrosion by the f-BNNS_{0.5}-PPy3/EP coating, which has the maximum corrosion potential ($E_{\rm corr}$) of -0.13 V. This was calculated from the potentiodynamic polarization data, which is displayed in the Tafel curves in Figure 13e. As a result, the corrosion rate ($V_{\rm corr}$) and

corrosion current density ($i_{\rm corr}$) of f-BNNS_{0.5}-PPy3/EP are 15 nm/year and 1.3×10^{-9} A·cm⁻², respectively, which are about an order a factor less compared to that of the f-BNNS0.5/EP coating. These findings confirm that adding polypyrrole to the f-BNNS-epoxy composite increases its corrosion barrier, which in turn prevents invading species. Also, the electrochemical comparison of hBN, carbon nitrides, polyurethane/GO, and silane-functionalized RuO₂ nanoparticles also provides a clear understanding of different polymeric coatings with respect to their anticorrosion properties [105–107]. Further, Table 3 compares the electrochemical properties of BNNSs in various composite materials.

Table 3: Comparison of electrochemical parameters of BNNSs of various composites [45,99,101]

Composite materials	Parameters		
	E _{cor} (V)	$I_{\rm cor}$ (A·cm $^{-2}$)	
BNNS in polypyrrole	-0.13	1.3 × 10 ⁻⁹	
BNNS in acrylic	-1.06	2.3×10^{-7}	
Phosphate-treated BNNS	-0.44	1.5×10^{-5}	
BNNS in acrylic	-0.57	3.8×10^{-6}	

2.4 Anticorrosion mechanism

Anticorrosion mechanisms are processes or techniques that are proposed in regard to preventing or impairing the corrosion of materials, such as metals and alloys that are exposed to severe environments. Corrosion is the degradation/deterioration of metal due to a chemical reaction in an ambient environment. Oxygen and moisture typically play an important role in this reaction, which leads to the formation of oxides, hydroxides, or sulfides. Anticorrosion mechanisms are decisive in extending the aging factor of materials and alloys to retain the integrity of the structure and fatigue behavior [108].

Figure 14 shows the schematic representation of the corrosion protection mechanism of the PDA-BN@ZnO coating. The hBN is coated with PDA by adding ZnO ions *via* a hydrothermal technique. The whole coating functions as a barrier to

effectively block the corrosive liquid from penetrating during the initial immersion stage. Nonetheless, imperfections, such as holes and microcracks, are unavoidable with polymer coatings. The corrosive medium eventually penetrates through the pores of the coating as the immersion duration rises. The PDA-BN@ZnO nano-pigment is compatible with the silicon-epoxy (SE) matrix, and it improves the interfacial contact by chemical bonding (Zn–O–Si). This allows the penetration route to be expanded for the corrosive media and the composite coating's barrier effectiveness to be enhanced, which improves the passive impermeability. Moreover, PDA-BN@Zn²⁺ has a particular capture impact on the Cl⁻ ion during its penetration. As a result, the process of charge neutralization is hampered by a reduction in the amount of freed Cl⁻ in the electrochemical erosion of the Al-alloy substrate.

In addition, an electrochemical corrosion process at the coating/Al-alloy interaction releases PDA and Zn²⁺ ions in an acid–base environment. An Al³⁺–PDA complex is formed when the released PDA moves to the anode area and anchors Al³⁺. Zn²⁺ gets absorbed at the cathode area where they precipitate zinc hydroxide, which inhibits the cathode reaction, under the influence of the H⁺ that is generated by the anode reaction. Favorable corrosion inhibition is demonstrated by PDA and Zn²⁺, which reduces metal corrosion and provides a positive active protective effect. The PDA-BN@ZnO/SE coating has superior long-term anticorrosive capabilities when compared to the other nano-pigment-enhanced anticorrosive coatings. PDA-BN@ZnO nano-pigments may

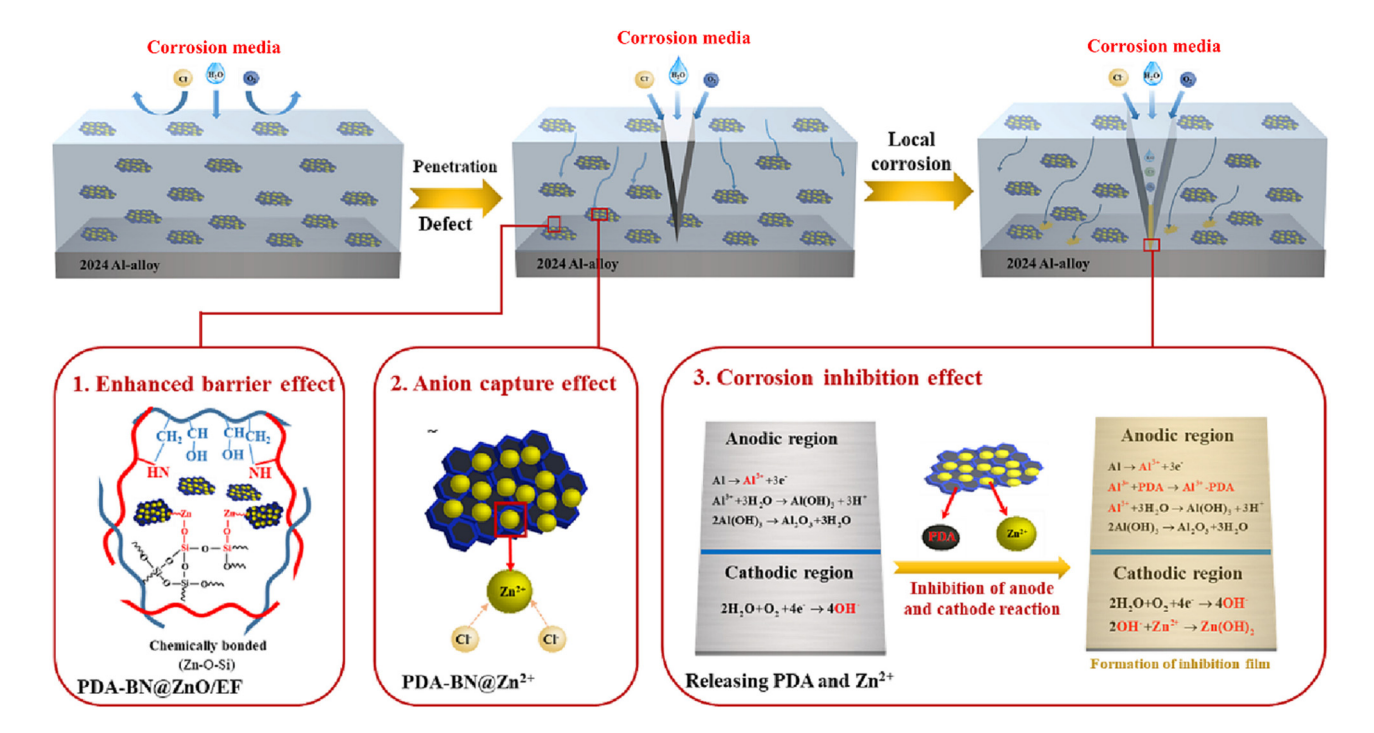


Figure 14: Illustration of the PDA-BN@ZnO/SE coating's protective mechanism [97].

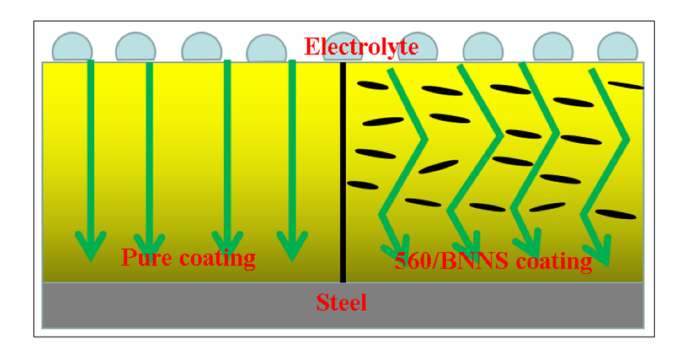


Figure 15: Schematic illustration of a corrosion inhabitation mechanism [45].

consequently be used to construct high-performance and longterm protective coatings with good barrier, chlorine capture, and corrosion inhibition effects as well as to greatly improve the protective qualities of SE coatings [97].

The addition of 560/BNNS can increase the corrosion resistance of acrylic coatings on galvanized steel. Figure 15 shows the corrosion inhabitation mechanism of 560/BNNS. The BNNS nanosheets are evenly dispersed throughout the aqueous acrylic coating, and they make the mutual interfacial crosslinking of organic molecules. The coating was also made smooth and uniform, since 560/BNNSs were impermeable due to the better interfacial interaction. The crack propagation can be efficiently controlled by crosslinking using silane membranes. These findings demonstrate that the number of fractures significantly decreased when the organic coatings dried. These effects allow the production of a relatively thick and complete coating, which improves the barrier of the material. This morphology of the 560/BNNS/waterborne acrylic and BNNS/waterborne acrylic coatings also improved the corrosion protection. The ion interaction between the solution and the metal substrate may be effectively inhibited, and the diffusion of the ion channel can be extended through the addition of BNNS and 560/BNNS to the waterborne acrylic solution. The corrosion resistance of the composite coating consequently increased and its rate of corrosion for galvanized steel decreased [45].

2.5 Comparison of BNNS with other materials for corrosion-resistance coating

The BNNS is significantly used in organic coating to embark the anticorrosive properties which have a great impact on the passivating performance of hBN composite coating [20]. But BNNSs have a few issues of uniform dispersion, interface interaction, and antifriction properties with organic resins in the organic coating, so such limitations deteriorate the protection performance of the composite coating in industrial applications [109,110]. Therefore, surface doping and adaptation can enhance the interface interaction and dispersion uniformity of BNNS in organic resins while making composites with other materials for great commercial benefits [111,112]. On the other hand, regardless of BNNS and its surface modification, a few promising nanocomposite materials including graphene oxide, polyacrylamide/TiO2, and silanized cerium carbide nanofillers also improve the structural and mechanical features of epoxy coating for automotive applications [113-115]. Overall, the actual mechanisms of phase transition across the interphase between hBN and other matrix-based composites during crystallization are not well addressed. Consequently, the deep understanding of interactions at the heterointerface between hBN and organic phase change materials, mainly in the context of corrosion resistance coating, can lead to advancements in materials science.

2.6 Environmental and health impact of hBN and BNNS

2.6.1 Environmental impact

In this section, the synthesis of BNNS and their potential impact on the environment and human health are addressed. BNNSs are attracting a huge amount of attention due to their rare properties of excellent thermal conductivity and high mechanical strength. They are being used in many applications, electronics circuits, coatings, and high-density energy storage devices. However, the production and application of BNNS also have some environmental and health issues, like other nanomaterials. For example, raw material extraction (boron) through mining, synthesis processing at high temperatures, chemical usage during the production process, and the generation of waste are notorious challenges to deal with due to their possible toxicity and persistence in the environment [116]. A recent investigation revealed that no data have been found for hBN, but single boron could be the least toxic among 36 metals metalloids in an ostracod Cypris subglobosa aquatic system [117]. A recent report in Italy demonstrated no environmental risk effects of boron in groundwaters by applying Daphnia as an ecotoxicology readout [118]. However, a 3-year finding that was conducted on a Canadian oil end pit lake found that boron exhibits a very high toxicological risk to aquatic organisms, which can be carefully managed by adopting green production methods

and improving life-cycle management to ensure innocuous BNNS for clean and green environment [119].

2.6.2 Health impact

The toxic effect of hBN on the human body at the skin level is still elusive, and no *in vivo* studies have been accomplished yet to assess the cutaneous effects of hBN. However, the Cosmetic Ingredient Review Expert Panel reported a safety assessment of hBN (50% hBN in olive oil) used in cosmetics as a slip modifier in 2015, which is not an irritant to the body skin. In addition, face powder and eye shadow formulations that contain hBN (13–18%) were also non-irritant and non-sensitizing for the skin. All these findings were supported by unpublished results that were provided by the Personal Care Products Council without any experimental information on physicochemical properties of the tested materials [120].

Furthermore, a few *in vivo* studies of hBN and hBN nanotubes have been established thus far [121,122]. Liu *et al.* studied the toxicity of polyethylene glycol (PEG) coated hBN (20 mg·kg⁻¹) in mice in 2015 which accumulated in the liver, lung, heart, and spleen [123]. It was notably observed that a biodistribution of BN-PEG in the heart with high toxicity could be a risk of cardiovascular disease. Nonetheless, BN is being used in many typical cosmetics products, and they found it to be harmless in the specific quantity that was used even if it was inhaled [124]. Various other 2D materials, such as hBN, can be used for the treatment of brain tumor imaging with the careful safety assessment and close monitoring that are required to the degradability of the materials.

3 Future perspectives

The future prospect of the hBN and BNNSs in anti-corrosion coatings is indispensable, and the human health and environmental concerns cannot be avoided in this endeavor, which is provided as follows.

- 1) There are several ways to synthesize BNNSs, and each of them has its own benefits and drawbacks. For instance, CVD can be costly, and liquid exfoliation reagents can be hazardous. It is therefore important to investigate more effective, economical, and environmentally friendly techniques, such as microwaveassisted and electrochemical exfoliation to enhance the production and quality of BNNSs as well as lower the pollution and energy usage.
- 2) Improving the ordered arrangement of BNNSs in protective coatings presents another important area for

future study. The ordered arrangement of BNNSs in a coating matrix, which was opposed to random alignment, is more favorable for extending the penetration route and boosting the ability of coating to hold the penetration of corrosive chemicals. BNNSs with ordered alignments in coatings were produced in some studies. However, a thorough and in-depth investigation of the process behind the orderly distribution of BNNSs in coatings has not yet been conducted. More accurate and tunable directional control techniques in conjunction with more effective and mild dispersion techniques are required because the dispersion process of BNNSs cannot be efficiently controlled.

- 3) BNNS composite coatings still have several limitations to overcome the issues of industrial applications. For instance, more affordable, eco-friendly, and effective preparation techniques must be established, because the recent BNNS preparation method is quite expensive. Second, modifying the surface technology and dispersant selection need to be optimized, and the dispersion homogeneity of BNNSs in polymers must be enhanced. Third, the coating preparation procedure and interface treatment technique need to be enhanced, because the degree of bonding of hBN nanocomposite coatings and metallic substrates is not optimal. Finally, the primary emphasis of the current research is on how hBN nanocomposite coatings behave during short-term corrosion in a lab setting. The long-term stability and durability of additional accelerated aging studies and real-world application testing must be conducted prior to the hBN coating of a nanocomposite to confirm the longterm stability and endurance of hBN nanocomposite coatings under various environmental conditions.
- 4) It is important to note that the relation between 2D materials and biological systems is contingent. 2D materials may consequently have a great influence on the cells and tissues of living organisms, which initiate toxicity, but biological systems can prevent this effect through enzymatic degradation. This essentially has been exhibited in the environment and mammalian systems. It is therefore vital to develop and employ an effective testing tool by using robust model systems to ensure the safety of human health and the environment.

4 Conclusions

In summary, we emphasized the significance and diversity of hBN as a promising material for corrosion protection coatings and its impact on ecological and healthcare monitoring. However, it is elucidated that by incorporating hBN into organic coatings, researchers have overcome several drawbacks. The exceptional properties of hBN, which include high hardness, oxidation resistance, and barrier protection, make it an ideal candidate for corrosion protection applications. This review concludes that hBN coatings improve corrosion resistance, hydrophobicity, and crack mitigation properties, which offer a viable solution to the challenges that are faced by conventional materials and their coating methods. Furthermore, this study explicitly highlighted the concerns of toxicity and the environmental and health risks due to BNNS production and their applications of corrosion protection. Finally, we summarized the prospects of hBN for advanced corrosion protection technologies while controlling the toxic and hazards effects on the environment and health.

DE GRUYTER

Acknowledgments: The authors extend their appreciation to the Deanship of Research and Graduate Studies at King Khalid University for funding this work through the Large Research Project under grant number RGP2/236/45. This study is also supported by the Basic Science Research Program via the National Research Foundation of Korea (NRF), Grant no. 2022R1F1A1075229.

Funding information: This work was funded by the Deanship of Research and Graduate Studies at King Khalid University through the Large Research Project under grant number RGP2/236/45. This study is also supported by the Basic Science Research Program via the National Research Foundation of Korea (NRF), Grant no. (2022R1F1A1075229).

Author contributions: All authors have accepted responsibility for the entire content of this manuscript and approved its submission.

Conflict of interest: The authors state no conflict of interest.

Data availability statement: The datasets generated and/ or analyzed during the current study are available from the corresponding author on reasonable request.

References

Yan, Y., K. Liao, J. Hu, M. Qin, T. He, T. Ou, et al. Effects of h-BN [1] content and silane functionalization on thermal conductivity and

- corrosion resistance of h-BN/EPN coating. Surface and Coatings Technology, Vol. 476, 2024, id. 130185.
- [2] Wang, W., W. Zhao, W. Mu, Z. Li, Z. Weng, W. Zhang, et al. Effect of hot-rolling process on the microstructure, mechanical and corrosion behaviors of dual-phase Co-based entropic alloys. Materials Science and Engineering: A, Vol. 918, 2024, id. 147433.
- Majeed, M. N., Q. A. Yousif, and M. A. Bedair. Study of the corrosion of nickel-chromium alloy in an acidic solution protected by nickel nanoparticles. ACS Omega, Vol. 7, 2022, pp. 29850-29857.
- [4] Nadeem, A., M. F. Maqsood, M. A. Raza, M. R. Karim, F. Ghafoor, Y. Lee, et al. Thermally stable and anti-corrosive polydimethyl siloxane composite coatings based on nanoforms of boron nitride. Inorganic Chemistry Communications, Vol. 168, 2024, id. 112989.
- Magsood, M. F., U. Latif, S. M. Z. Mehdi, Z. U. Rehman, M. A. Raza, [5] F. Ghafoor, et al. Effect of "Mn" substitution at B-site, on the crystal structure and energy storage performance of the La0. 75Sr0. 25CoO3 perovskite. Journal of Industrial and Engineering Chemistry, Vol. 139, 2024, pp. 587-600.
- [6] Kuklik, V. and J. Kudlacek. Hot-dip galvanizing of steel structures, Butterworth-Heinemann, Oxford, 2016, pp. 7-16.
- Wang JW, K., T. Zhang, and S. Wang. Key aspects of a DN4000 [7] steel pipe jacking project in China: A case study of a water pipeline in the Shanghai Huangpu River. Tunnelling and Underground Space Technology, Vol. 72, 2018, pp. 323-332.
- Meinert, K. C. U. and G. K. J. Matschullat. Wolf Corrosion and leaching of silver doped ceramic IBAD coatings on SS 316L under simulated physiological conditions. Surface and Coatings Technology, Vol. 103, 1998, pp. 58-65.
- [9] Bierwagen, G. P. Reflections on corrosion control by organic coatings. Progress in Organic Coatings, Vol. 28, 1996,
- Khan, M. H., H. K. Liu, X. Sun, Y. Yamauchi, Y. Bando, D. Golberg, et al. Few-atomic-layered hexagonal boron nitride: CVD growth, characterization, and applications. Materials Today, Vol. 20, 2017, pp. 611-628.
- [11] Li, X., G. Wang, and X. Li. Surface modifification of nano-SiO2 particles using polyaniline. Surface and Coatings Technology, Vol. 197, 2005, pp. 56-60.
- [12] Yang, M. L., J. L. Xu, J. Huang, L. W. Zhang, and J. M. Luo. Wear resistance of N-doped CoCrFeNiMn high entropy alloy coating on the Ti-6Al-4V alloy. Journal of Thermal Spray Technology, Vol. 33, 2024, pp. 2408-2418.
- [13] Ma, Z. S., H. L. Liu, Z. Liu, and Z. L. Cheng. Preparation and tribological properties of hydrothermally exfoliated ultrathin hexagonal boron nitride nanosheets (BNNSs) in mixed NaOH/ KOH solution. Journal of Alloys and Compounds, Vol. 784, 2019, pp. 807-815.
- [14] Lin, Z., W. Zhang, W. Zhang, L. Xu, Y. Xue, and W. Li. Fabrication of Ni-Co/Cu super-hydrophobic coating with improved corrosion resistance. Materials Chemistry and Physics, Vol. 277, 2022, id. 125503.
- [15] Shao, L., N. Xue, W. Li, S. Liu, Z. Tu, Y. Chen, et al. Effect of coldspray parameters on surface roughness, thickness and adhesion of copper-based composite coating on aluminum alloy 6061 T6 substrate. Processes, Vol. 11, 2023, id. 959.
- [16] Oliveira, R., J. Gonçalves, M. Ueda, S. Oswald, and S. Baldissera. Improved corrosion resistance of tool steel H13 by means of cadmium ion implantation and deposition. Surface and Coatings Technology, Vol. 204, 2010, pp. 2981-2985.

- [17] Chasse, K. R., A. J. Scardino, and G. W. Swain. Corrosion and fouling study of copper-based antifouling coatings on 5083 aluminum alloy. *Progress in Organic Coatings*, Vol. 141, 2020, id. 105555.
- [18] Wu, B., S. Lu, W. Xu, S. Cui, J. Li, and P. Han. Study on corrosion resistance and photocatalysis of cobalt superhydrophobic coating on aluminum substrate. *Surface and Coatings Technology*, Vol. 330, 2017. pp. 42–52.
- [19] He, G., H. Li, Z. Zhao, Q. Liu, J. Yu, Z. Ji, et al. Antifouling coatings based on the synergistic action of biogenic antimicrobial agents and low surface energy silicone resins and their application to marine aquaculture nets. *Progress in Organic Coatings*, Vol. 195, 2024. id. 108656.
- [20] Cui, M., S. Ren, J. Chen, S. Liu, G. Zhang, H. Zhao, et al. Anticorrosive performance of waterborne epoxy coatings containing water-dispersible hexagonal boron nitride (h-BN) nanosheets. *Applied Surface Science*, Vol. 397, 2017, pp. 77–86.
- [21] Nine, M. J., M. A. Cole, D. N. Tran, and D. Losic. Graphene: A multipurpose material for protective coatings. *Journal of Materials Chemistry A: Materials for Energy and Sustainability*, Vol. 3, 2015, pp. 12580–12602.
- [22] Maqsood, M. F., M. A. Raza, Z. U. Rehman, A. Tayyeb, M. A. Makhdoom, F. Ghafoor, et al. Role of solvent used in development of graphene oxide coating on AZ31B magnesium alloy: Corrosion behavior and biocompatibility analysis. *Nanomaterials*, Vol. 12, 2022. id. 3745.
- [23] Sun, W., L. Wang, T. Wu, Y. Pan, and G. Liu. Synthesis of lowelectrical-conductivity graphene/pernigraniline composites and their application in corrosion protection. *Carbon*, Vol. 79, 2014, pp. 605–614.
- [24] Yang, M., J. Wu, D. Fang, B. Li, and Y. Yang. Corrosion protection of waterborne epoxy containing mussel-inspired adhesive polymers based on polyaspartamide derivatives on carbon steel. *Journal of Materials Science & Technology*, Vol. 34, No. 12, 2018, pp. 2464–2471.
- [25] Maqsood, M. F., U. Latif, Z. A. Sheikh, M. Abubakr, S. Rehman, K. Khan, et al. A comprehensive study of Bi2Sr2Co2Oy misfit layered oxide as a supercapacitor electrode material. *Inorganic Chemistry Communications*, Vol. 158, 2023, id. 111487.
- [26] Khun, N. W., E. Liu, and X. T. Zeng. Corrosion behavior of nitrogen doped diamond-like carbon thin fifilms in NaCl solutions. *Corrosion Science*, Vol. 51, 2009, pp. 2158–2164.
- [27] Choudhury, N. R., A. G. Kannan, and N. K. Dutta. Novel nanocomposites and hybrids for lubricating coating applications. *Tribology and Interface Engineering Series*, Vol. 55, 2005, pp. 501–542.
- [28] Izadi, M., T. Shahrabi, and B. Ramezanzadeh. Active corrosion protection performance of an epoxy coating applied on the mild steel modified with an eco-friendly sol-gel film impregnated with green corrosion inhibitor loaded nanocontainers. *Applied Surface Science*, Vol. 440, 2018, pp. 491–505.
- [29] Lu, F., C. Liu, Z. Chen, U. Veerabagu, Z. Chen, M. Liu, et al. Polypyrrole-functionalized boron nitride nanosheets for highperformance anti-corrosion composite coating. *Surface and Coatings Technology*, Vol. 420, 2021, id. 127273.
- [30] Mariz, IFA, I. S. Millichamp, J. C. de la Cal, and J. R. Leiza. High performance water-borne paints with high volume solids based on bimodal latexes. *Progress in Organic Coatings*, Vol. 68, 2010, pp. 225–233.

- [31] Karger-Kocsis, J. Paints, coatings and solvents. Composites Science and Technology, Vol. 51, 1994, pp. 613–614.
- [32] Forsgren, A. Corrosion control through organic coatings, Corrosion Technology, CRC Press, Taylor & Francis Group, Boca Raton, 2006.
- [33] Yu, F., X. Xu, N. Lin, and X. Y. Liu. Structural engineering of waterborne polyurethane for high performance waterproof coatings. RSC Advances, Vol. 5, 2015, pp. 72544–72552.
- [34] Xavier, J. R. Superior barrier, hydrophobic, and mechanical properties of the epoxy nanocomposite containing mixed metal oxides. *Journal of Adhesion Science and Technology*, Vol. 37, 2023, pp. 1394–1418.
- [35] Xavier, J. R. Superior corrosion protection performance of polypdopamine-intercalated CeO 2/polyurethane nanocomposite coatings on steel in 3.5% NaCl solution. *Journal of Applied Electrochemistry*, Vol. 51, 2021, pp. 959–975.
- [36] Xavier, J. R. and S. Vinodhini. Investigation into the effect of introducing functionalized hafnium carbide with GO in the epoxy coated aluminium alloy for aerospace components. *Colloids and Surfaces, A: Physicochemical and Engineering Aspects*, Vol. 658, 2023, id. 130667.
- [37] Xavier, J. R. and B. Ramesh. A study on the effect of multifunctional tantalum carbide nanofillers incorporated graphene oxide structure in the epoxy resin for the applications in the shipbuilding industry. *Materials Science and Engineering: B*, Vol. 289, 2023, id. 116234.
- [38] Huang, W., D. Mei, Y. Zhong, J. Li, S. Zhu, Y. Chen, et al. The enhanced antibacterial effect of BNNS_Van@ CS/MAO coating on Mg alloy for orthopedic applications. *Colloids and Surfaces B: Biointerfaces*, Vol. 221, 2023, id. 112971.
- [39] Nair, R. M., B. Bindhu, and R. R. Isaac. Boron nitride nanosheets dispersed biopolymer solution as an effective copper corrosion inhibitor in acidic medium. *Polymer Bulletin*, Vol. 80, 2023, pp. 12849–12863.
- [40] Verma, C., S. Dubey, I. Barsoum, A. Alfantazi, E. E. Ebenso, and M. Quraishi. Hexagonal boron nitride as a cutting-edge 2D material for additive application in anticorrosive coatings: recent progress, challenges and opportunities. *Materials Today Communications*, Vol. 35, 2023, id. 106367.
- [41] Wan, S., H. Chen, G. Cai, B. Liao, and X. Guo. Functionalization of h-BN by the exfoliation and modification of carbon dots for enhancing corrosion resistance of waterborne epoxy coating. *Progress in Organic Coatings*, Vol. 165, 2022, id. 106757.
- [42] Yan, Y., X. Jiang, K. Liao, J. Leng, M. Qin, X. Lyu, et al. Effects of OCF content and oxidation treatment on thermal conductivity and corrosion resistance of CF/BN/EPN coating. Surface and Coatings Technology, Vol. 481, 2024, id. 130664.
- [43] Wan, S., H. Chen, B. Liao, and X. Guo. Enhanced anti-corrosive capability of waterborne epoxy coating by ATT exfoliated boron nitride nanosheets composite fillers. *Progress in Organic Coatings*, Vol. 186, 2024, id. 108089.
- [44] Sun, X., J. Zhang, W. Pan, W. Wang, and C. Tang. A review on the preparation and application of BN composite coatings. *Ceramics International*, Vol. 49, 2023, pp. 24–39.
- [45] Xu, X., S. Zhang, Y. Wang, N. Wang, Q. Jiang, X. Liu, et al. 2D surfaces twisted to enhance electron freedom toward efficient advanced oxidation processes. *Applied Catalysis B: Environment* and Energy, Vol. 345, 2024, id. 123701.
- [46] Petrescu, M. I. Boron nitride theoretical hardness compared to carbon polymorphs. *Diamond and Related Materials*, Vol. 13, 2004, pp. 1848–1853.

- Wan, S., H. Chen, X. Ma, L. Chen, K. Lei, B. Liao, et al. Anticorrosive reinforcement of waterborne epoxy coating on Q235 steel using NZ/BNNS nanocomposites. Progress in Organic Coatings, Vol. 159, 2021, id. 106410.
- [48] Nadeem, A., M. F. Maqsood, M. A. Raza, M. T. Ilyas, M. J. Iqbal, and Z. U. Rehman. Binder free boron nitride-based coatings deposited on mild steel by chemical vapour deposition: Anti-corrosion performance analysis. Physica B: Condensed Matter, Vol. 602, 2021, id 412600
- Wang, L., G. Wang, Y. Di, H. Wang, P. Wang, L. Dong, et al. Fast reversion of hydrophility-superhydrophobicity on textured metal surface by electron beam irradiation. Applied Surface Science, 2024. id. 160455.
- [50] Nekouee, K., F. Moravvei, M. Amishi, and S. Abbasalizade. Synthesis and characterization of h-boron nitride by urea routes, 2021.
- [51] Naclerio, A. E. and P. R. Kidambi. A review of scalable hexagonal boron nitride (h-BN) synthesis for present and future applications. Advanced Materials, Vol. 35, 2023, id. 2207374.
- [52] Román, R. J. P., F. J. C. Costa, A. Zobelli, C. Elias, P. Valvin, G. Cassabois, et al. Band gap measurements of monolayer h-BN and insights into carbon-related point defects. 2D Materials, Vol. 8, 2021, id. 044001.
- [53] Lipp, A., K. A. Schwetz, and K. Hunold. Hexagonal boron nitride: fabrication, properties and applications. Journal of the European Ceramic Society, Vol. 5, No. 1, 1989, pp. 3-9.
- [54] Zhao, L.-H., L. Wang, Y.-F. Jin, J.-W. Ren, Z. Wang, and L.-C. Jia. Simultaneously improved thermal conductivity and mechanical properties of boron nitride nanosheets/aramid nanofiber films by constructing multilayer gradient structure. Composites, Part B: Engineering, Vol. 229, 2022, id. 109454.
- Li, C. Thickness-dependent bending modulus of hexagonal boron nitride nanosheets. Nanotechnology, Vol. 20, No. 38, 2009, id. 385707.
- [56] Golberg, D. Boron nitride nanotubes and nanosheets. Nano Letters ACS, Vol. 4, No. 6, 2010, pp. 2979-2993.
- [57] Ouyang, T. Thermal transport in hexagonal boron nitride nanoribbons. Nanotechnology, Vol. 21, No. 24, 2010, id. 245701.
- liang, X. F. Recent progress on fabrications and applications of boron nitride nanomaterials: a review. Journal of Materials Science & Technology, Vol. 31, 2015, pp. 589-598.
- Yi, M., Z. Shen, X. Zhao, S. Liang, and L. Liu. Boron nitride [59] nanosheets as oxygen-atom corrosion protective coatings. Applied Physics Letters, Vol. 104, 2014, id. 143101.
- Jeeva, N., K. Thirunavukkarasu, and J. R. Xavier. Influence of multifunctional graphene oxide and silanized vanadium nitride in polyurethane coatings for the protection of aluminium alloy in aerospace industries. Diamond and Related Materials, Vol. 142, 2024, id. 110792.
- Xavier, J. R. and N. Jeeva. Evaluation of newly synthesized nanocomposites containing thiazole modified aluminium nitride nanoparticles for aerospace applications. Materials Chemistry and Physics, Vol. 286, 2022, id. 126200.
- Xavier, J. R. and Jeeva N. Effects of incorporation of silanized [62] titanium nitride on the electrochemical and mechanical properties of polyurethane in aircraft coating. Journal of Polymer Research, Vol. 29, 2022, id. 305.
- Ertuğ, B. Powder preparation, properties and industrial applications of hexagonal boron nitride. Sintering Applications, Vol. 33, 2013, pp. 1-352.

- [64] Aldinger, S., U. Herzog, B. Jäschke, T. Jäschke, E. Müller, G. Roewer, et al. High performance non-oxide ceramics I, Springer-Verlag Berlin, Heidelberg, Germany, 2003.
- [65] Sharma, V., H. L. Kagdada, P. K. Jha, P. Śpiewak, and K. J. Kurzydłowski. Thermal transport properties of boron nitride based materials: A review. Renewable and Sustainable Energy Reviews, Vol. 120, 2020, id. 109622.
- [66] Rathinasabapathy, S., M. S. Santhosh, and M. Asokan. Significance of boron nitride in composites and its applications. Recent advances in boron-containing materials, IntechOpen,
- [67] Arenal, R. and A. Lopez-Bezanilla. Boron nitride materials: an overview from 0D to 3D (nano)structures. WIREs Computational Molecular Science, Vol. 5, 2015, pp. 299-309.
- [68] Dunlop, M. J. and R. Bissessur. Nanocomposites based on graphene analogous materials and conducting polymers: a review. Journal of Materials Science, Vol. 55, 2020, pp. 6721-6753.
- [69] Qayyum, M. S., H. Hayat, R. K. Matharu, T. A. Tabish, and M. Edirisinghe. Boron nitride nanoscrolls: Structure, synthesis, and applications. Applied Physics Reviews, Vol. 6, 2019, id. 021310.
- Barth, J. V., G. Costantini, and K. Kern. Engineering atomic and [70] molecular nanostructures at surfaces. Nature, Vol. 437, 2005, pp. 671-679.
- [71] Mirzaee, M., A. Rashidi, A. Zolriasatein, and M. R. Abadchi. A simple, low cost, and template-free method for synthesis of boron nitride using different precursors. Ceramics International, Vol. 47, 2021, pp. 5977-5984.
- Yu, R. and X. Yuan. Rising of boron nitride: A review on boron [72] nitride nanosheets enhanced anti-corrosion coatings. Progress in Organic Coatings, Vol. 186, 2024, id. 107990.
- [73] Pan, D., F. Su, H. Liu, Y. Ma, R. Das, Q. Hu, et al. The properties and preparation methods of different boron nitride nanostructures and applications of related nanocomposites. The Chemical Record, Vol. 20, 2020, pp. 1314-1337.
- [74] Yang, G., H. Wang, N. Wang, R. Sun, and C.-P. Wong. Hydrothermal exfoliation for two-dimension boron nitride nanosheets. In Proceedings of 2018 IEEE 68th Electronic Components and Technology Conference (ECTC), IEEE, 2018.
- [75] Chen, C., L. He, C. Jiang, L. Chen, H. S. Wang, X. Wang, et al. Directional etching for high aspect ratio nano-trenches on hexagonal boron nitride by catalytic metal particles. 2D Materials, Vol. 9, 2022, id. 025015.
- [76] Pacile, D. The two-dimensional phase of boron nitride: Fewatomic-layer sheets and suspended membranes. Applied Physics Letters, Vol. 92, No. 13, 2008, id. 133107.
- [77] Meyer, J. C. Selective sputtering and atomic resolution imaging of atomically thin boron nitride membranes. Nano Letter, Vol. 9, No. 7, 2009, pp. 2683-2689.
- [78] Yu, L., P. L. Yap, D. N. Tran, A. M. Santos, and D. Losic. High-yield preparation of edge-functionalized and water dispersible fewlayers of hexagonal boron nitride (hBN) by direct wet chemical exfoliation. Nanotechnology, Vol. 32, 2021, id. 405601.
- [79] Mahdizadeh, A., S. Farhadi, and A. Zabardasti. Microwave-assisted rapid synthesis of graphene-analogue hexagonal boron nitride (h-BN) nanosheets and their application for the ultrafast and selective adsorption of cationic dyes from aqueous solutions. RSC Advances, Vol. 7, 2017, pp. 53984-53995.
- [80] Zhi, C., Y. Bando, C. Tang, H. Kuwahara, and D. Golberg. Largescale fabrication of boron nitride nanosheets and their utilization in polymeric composites with improved thermal and mechanical

- properties. *Advanced Materials*, Vol. 21, No. 28, 2009, pp. 2889–2893.
- [81] Wang, Y., Z. Shi, and J. Yin. Boron nitride nanosheets: large-scale exfoliation in methanesulfonic acid and their composites with polybenzimidazole. *Journal of Materials Chemistry*, Vol. 21, No. 30, 2011, pp. 11371–11377.
- [82] Marsh, K., M. Souliman, and R. B. Kaner. Co-solvent exfoliation and suspension of hexagonal boron nitride. *Chemical Communications*, Vol. 51, No. 1, 2015, pp. 187–190.
- [83] Thangasamy, P. and M. Sathish. Supercritical fluid processing: a rapid, one-pot exfoliation process for the production of surfactant-free hexagonal boron nitride nanosheets. *CrystEngComm*, Vol. 17, No. 31, 2015, pp. 5895–5899.
- [84] Gao, R., L. Yin, C. Wang, Y. Qi, N. Lun, L. Zhang, et al. High-yield synthesis of boron nitride nanosheets with strong ultraviolet cathodoluminescence emission. *The Journal of Physical Chemistry* C, Vol. 113, No. 34, 2009, pp. 15160–15165.
- [85] Nadeem, A., M. A. Raza, M. F. Maqsood, M. T. Ilyas, A. Westwood, and Z. U. Rehman. Characterization of boron nitride nanosheets synthesized by boron-ammonia reaction. *Ceramics International*, Vol. 46, No. 12, 2020, pp. 20415–20422.
- [86] Singhal, R., E. Echeverria, D. N. McIlroy, and R. N. Singh. Synthesis of hexagonal boron nitride films on silicon and sapphire substrates by low-pressure chemical vapor deposition. *Thin Solid Films*, Vol. 733, 2021, id. 138812.
- [87] Kumar, A., G. Malik, A. Kumar, R. Chandra, and R. S. Mulik. Transformation nanorod to nanotube of highly oriented novel h-BN hierarchical nanostructured arrays synthesized via two-step wet chemical route. *Materials Characterization*, Vol. 171, 2021, id. 110820.
- [88] Ghosh, B., F. Xu, D. M. Grant, P. Giangrande, C. Gerada, M. W. George, et al. Highly ordered BN⊥−BN⊥ stacking structure for improved thermally conductive polymer composites. Advanced Electronic Materials, Vol. 6, 2020, id. 2000627.
- [89] Fang, H., S.-L. Bai, and C. P. Wong. Thermal, mechanical and dielectric properties of flexible BN foam and BN nanosheets reinforced polymer composites for electronic packaging application. *Composites, Part A: Applied Science and Manufacturing*, Vol. 100, 2017, pp. 71–80.
- [90] Ren, J., L. Stagi, C. M. Carbonaro, L. Malfatti, M. F. Casula, P. C. Ricci, et al. Defect-assisted photoluminescence in hexagonal boron nitride nanosheets. 2D Materials, Vol. 7, 2020, id. 045023.
- [91] Raza, M. Effect of boron nitride addition on properties of vapour grown carbon nanofiber/rubbery epoxy composites for thermal interface applications. *Composites Science and Technology*, Vol. 120, 2015, pp. 9–16.
- [92] Rasul, M. G., A. Kiziltas, B. Arfaei, and R. Shahbazian-Yassar. 2D boron nitride nanosheets for polymer composite materials. npj 2D Materials and Applications, Vol. 5, 2021, id. 56.
- [93] Low, Z.-X., J. Ji, D. Blumenstock, Y.-M. Chew, D. Wolverson, and D. Mattia. Fouling resistant 2D boron nitride nanosheet–PES nanofiltration membranes. *Journal of Membrane Science*, Vol. 563, 2018, pp. 949–956.
- [94] Hong, Z., Y. Xing, M. Xue, D. Yang, Y. Luo, Z. Yin, et al. Excellent anti-fouling properties and high thermal conductivity of superhydrophobic SiC/PU-coated BNNS composite films. *Journal of Electronic Materials*, Vol. 53, 2024, pp. 6228–6242.
- [95] Li, L. H. Boron nitride nanosheets for metal protection. Advanced Materials Interfaces, Vol. 1, No. 8, 2014, id. 1300132.

- [96] Shan, Z., X. Jia, R. Tian, J. Yang, Y. Su, and H. Song. In-situ exfoliation of large sized h-BNNS by esterified nanocellulose to build aqueous lubricants that can switch between liquid and gel states. *Tribology International*, Vol. 188, 2023, id. 108843.
- [97] Liu, D., M. Zhang, L. He, Y. Chen, and W. Lei. Layer-by-layer assembly fabrication of porous boron nitride coated multifunctional materials for water cleaning. *Advanced Materials Interfaces*, Vol. 4, 2017, id. 1700392.
- [98] Ysiwata-Rivera, A. P., E. Hernández-Hernández, G. Cadenas-Pliego, C. A. Ávila-Orta, P. González-Morones, J. A. Velásquez-de Jesús, et al. Effect of modified hexagonal boron nitride nanoparticles on the emulsion stability, viscosity and electrochemical behavior of nanostructured acrylic coatings for the corrosion protection of AISI 304 stainless steel. *Coatings*, Vol. 10, 2020, id. 488.
- [99] Huang, H., H. Wang, Y. Xie, D. Dong, X. Jiang, and X. Zhang. Incorporation of boron nitride nanosheets in zinc phosphate coatings on mild steel to enhance corrosion resistance. *Surface and Coatings Technology*, Vol. 374, 2019, pp. 935–943.
- [100] Zhang, Z., H. Yuan, F. Qi, N. Zhao, B. Zhang, and X. Ouyang. Functionalized modified BN@F-SiC particle-incorporating epoxy: an effective hydrophobic antiwear and anticorrosion coating material. *Industrial & Engineering Chemistry Research*, Vol. 60, 2021, pp. 8430–8441.
- [101] Zou, B., X. Chang, J. Yang, S. Wang, J. Xu, S. Wang, et al. Plasma treated h-BN nanoflakes as barriers to enhance anticorrosion of acrylic coating on steel. *Progress in Organic Coatings*, Vol. 133, 2019, pp. 139–144.
- [102] Shen, L., Y. Zhao, Y. Wang, R. Song, Q. Yao, S. Chen, et al. A long-term corrosion barrier with an insulating boron nitride mono-layer. *Journal of Materials Chemistry A: Materials for Energy and Sustainability*, Vol. 4, 2016, pp. 5044–5050.
- [103] Wang, M., M. Liu, and J. Fu. An intelligent anticorrosion coating based on pH-responsive smart nanocontainers fabricated via a facile method for protection of carbon steel. *Journal of Materials Chemistry A: Materials for Energy and Sustainability*, Vol 3, 2015, pp. 6423–6431.
- [104] Fu, J., T. Chen, M. Wang, N. Yang, S. Li, Y. Wang, et al. Acid and alkaline dual stimuli-responsive mechanized hollow mesoporous silica nanoparticles as smart nanocontainers for intelligent anticorrosion coatings. ACS Nano, Vol. 7, 2013, pp. 11397–11408.
- [105] Xavier, J. R. and V. SP. Flame retardant and anticorrosion behavior of multifunctional epoxy nanocomposite coatings containing graphitic carbon nitride/silanized HfO2 nanofillers for the protection of steel surface in automobile industry. ACS Chemical Health & Safety, Vol. 30, 2023, pp. 428–450.
- [106] Xavier, J. R. Investigation of anticorrosion, flame retardant and mechanical properties of polyurethane/GO nanocomposites coated AJ62 Mg alloy for aerospace/automobile components. *Diamond and Related Materials*, Vol. 136, 2023, id. 110025.
- [107] Xavier, J. R., S. Vinodhini, and J. R. Beryl. Effect of silane-functionalized RuO2 nanoparticles on the anticorrosive and mechanical properties of poly (methyl methacrylate) coatings. *Metallurgical* and Materials Transactions A, Vol. 52, 2021, pp. 3896–3909.
- [108] Zhang, X. M., Z. Y. Chen, H. F. Luo, Z. Teng, Y. L. Zhao, and Z. C. Ling. Corrosion resistances of metallic materials in environments containing chloride ions: A review. *Transactions of Nonferrous Metals Society of China*, Vol. 32, 2022, pp. 377–410.
- [109] Wu, Y., Y. Wu, Y. Sun, W. Zhao, and L. Wang. 2D nanomaterials reinforced organic coatings for marine corrosion protection:

- State of the art, challenges, and future prospectives. *Advanced Materials*, Vol. 36, 2024, id. 2312460.
- [110] Li, J., L. Gan, Y. Liu, S. Mateti, W. Lei, Y. Chen, et al. Boron nitride nanosheets reinforced waterborne polyurethane coatings for improving corrosion resistance and antifriction properties. *European Polymer Journal*, Vol. 104, 2018, pp. 57–63.
- [111] Soong, Y.-C., J.-W. Li, Y.-F. Chen, J.-X. Chen, W. A. Lee Sanchez, W.-Y. Tsai, et al. Polymer-assisted dispersion of boron nitride/ graphene in a thermoplastic polyurethane hybrid for cooled smart clothes. ACS Omega, Vol. 6, 2021, pp. 28779–28787.
- [112] Wong, T. L., C. Vallés, A. Nasser, and C. Abeykoon. Effects of boron-nitride-based nanomaterials on the thermal properties of composite organic phase change materials: A state-of-the-art review. Renewable and Sustainable Energy Reviews, Vol. 187, 2023, id. 113730.
- [113] Vinodhini, S. and J. R. Xavier. Effect of graphene oxide wrapped functional silicon carbide on structural, surface protection, water repellent, and mechanical properties of epoxy matrix for automotive structural components. *Colloids and Surfaces, A: Physicochemical and Engineering Aspects*, Vol. 639, 2022, id. 128300.
- [114] Vinodhini, S. and J. R. Xavier. Investigation of anticorrosion and mechanical properties of azole functionalized graphene oxide encapsulated epoxy coatings on mild steel. *Journal of Failure Analysis and Prevention*, Vol. 21, 2021, pp. 649–661.
- [115] Xavier, J. R. and B. Ramesh. Experimental investigation of polymer matrix filled with silanized cerium carbide nanofillers and graphene oxide in automotive components. *Applied Nanoscience*, Vol. 13, 2023, pp. 6133–6149.
- [116] Lin, H., T. Buerki-Thurnherr, J. Kaur, P. Wick, M. Pelin, A. Tubaro, et al. Environmental and health impacts of graphene and other two-dimensional materials: a graphene flagship perspective. ACS Nano, Vol. 18, 2024, pp. 6038–6094.

- [117] Khangarot, B. and S. Das. Acute toxicity of metals and reference toxicants to a freshwater ostracod, Cypris subglobosa Sowerby, 1840 and correlation to EC50 values of other test models. *Journal of Hazardous Materials*, Vol. 172, 2009, pp. 641–649.
- [118] Gonçalves, S. F., A. R. R. Silva, M. D. Pavlaki, R. G. Morgado, and S. Loureiro. Site-specific hazard evaluation for improved groundwater risk assessment. *Chemosphere*, Vol. 274, 2021, id. 129742.
- [119] White, K. B. and K. Liber. Early chemical and toxicological risk characterization of inorganic constituents in surface water from the Canadian oil sands first large-scale end pit lake. *Chemosphere*, Vol. 211, 2018, pp. 745–757.
- [120] Fiume, M. M., W. F. Bergfeld, D. V. Belsito, R. A. Hill, C. D. Klaassen, D. C. Liebler, et al. Safety assessment of boron nitride as used in cosmetics. *International Journal of Toxicology*, Vol. 34, 2015, pp. 53S–60S.
- [121] Kodali, V. K., J. R. Roberts, M. Shoeb, M. G. Wolfarth, L. Bishop, T. Eye, et al. Acute in vitro and in vivo toxicity of a commercial grade boron nitride nanotube mixture. *Nanotoxicology*, Vol. 11, 2017, pp. 1040–1058.
- [122] Kodali, V., J. R. Roberts, E. Glassford, R. Gill, S. Friend, K. L. Dunn, et al. Understanding toxicity associated with boron nitride nanotubes: Review of toxicity studies, exposure assessment at manufacturing facilities, and read-across. *Journal of Materials Research*, Vol. 37, 2022, pp. 4620–4638.
- [123] Liu, B., W. Qi, L. Tian, Z. Li, G. Miao, W. An, et al. In vivo biodistribution and toxicity of highly soluble PEG-coated boron nitride in mice. *Nanoscale Research Letters*, Vol. 10, 2015, pp. 1–7.
- [124] Domi, B., K. Bhorkar, C. Rumbo, L. Sygellou, S. N. Yannopoulos, R. Barros, et al. Assessment of physico-chemical and toxicological properties of commercial 2D boron nitride nanopowder and nanoplatelets. *International Journal of Molecular Sciences*, Vol. 22, 2021, id. 567.